Assessing the impact of the environmental contamination on the transmission of Ebola Virus Disease (EVD)

Berge Tsanou · Jean Lubuma · Samuel Bowong · Joseph Mbang

Abstract This paper deals with the following biological question: *how influential is the environmental contamination on the transmission of EVD?* Based on the works in [7,33,55], we design a new mathematical model to address this question by assessing the effect of the Ebola virus contaminated environment on the dynamical transmission of EVD. The formulated model captures two infection pathways through both direct human-to-human transmission and indirect human-to-environment-to-human transmission by incorporating the environment as a transition and/or reservoir of Ebola viruses. We compute the basic reproduction number $\mathcal{R}_0^{env}$ for the model with environmental contamination and prove that the disease-free equilibrium is globally asymptotically stable (GAS) whenever $\mathcal{R}_0^{env} \leq 1$. When $\mathcal{R}_0^{env} > 1$, we show that the said model has a unique endemic equilibrium which is GAS. Similar results hold for the free environmental contamination sub-model (without the incorporation of the indirect transmission). More precisely, for the latter model, calculate the corresponding basic reproduction number $\mathcal{R}_0^h$ and establish the GAS of the disease-free and endemic equilibria, whenever $\mathcal{R}_0^h \leq 1$ and $\mathcal{R}_0^h > 1$, respectively. At the endemic level, we show that the number of infected individuals for the full model with the environmental contamination is greater than the corresponding number for the free environmental contamination sub-model. In conjunction with the inequality $\mathcal{R}_0^h < \mathcal{R}_0^{env}$, our finding suggests a negative answer to the biological question under investigation, i.e. the contaminated environment plays a detrimental role on the transmission dynamics of EVD by increasing the endemic level and/or the severity of the outbreak. Therefore, it is natural to implement a control strategy which aim at reducing the severity of the disease by providing adequate hygienic living conditions, educate populations at risk to follow rigorously those basic hy-

Berge Tsanou[1,2,5,6]
[1] Department of Mathematics and Computer Science, University of Dschang, P.O. Box 67 Dschang, Cameroon
[5] IRD UMI 209 UMMISCO, University of Yaounde I, P.O. Box 337 Yaounde, Cameroon
[6] LIRIMA-GRIMCAPE Team Project, University of Yaounde I, P.O. Box 812 Yaounde, Cameroon

Tel.: +237 681 839 229
E-mail: bergetsanou@yahoo.fr ; berge.tsanou@univ-dschang.org
Present address: Department of Mathematics and Applied Mathematics, University of Pretoria, Pretoria 0002, South Africa

Jean Lubuma[2]
[2] Department of Mathematics and Applied Mathematics, University of Pretoria, Pretoria 0002, South Africa

Samuel Bowong[3,5,6]
[3] Department of Mathematics and Computer Science, University of Douala, P.O. Box 24157 Douala, Cameroon

Joseph Mbang[4,5,6]
[4] Department of Mathematics, Faculty of Science, University of Yaounde I, P.O. Box 812 Yaounde, Cameroon

gienic conditions as well as ask them avoid contact with suspected contaminated objects. Further, we perform numerical simulations to support the theory.

Keywords Ebola, Reservoir · Environmental transmission · Dynamical system · Stability.

Mathematics Subject Classification (2000) 92A15 · 34D20 · 37B25

1 Introduction

The Ebola Virus Disease (EVD) is caused by infection with a virus of the family Filoviridae, genus Ebolavirus. The Ebola virus was first associated with an outbreak the Democratic Republic of Congo: DRC (former Zaire) in 1976. Since then many other outbreaks have occurred mainly in Central Africa. The 2014-2015 outbreak in West Africa is by far the largest outbreak of Ebola virus disease ever recorded with the Zaire species of the virus [5, 23,53,54]. By October 2014, a total number of 9286 confirmed, probable and suspected cases of EVD have been reported in eight affected countries worldwide: DRC (70) Guinea (1519), Liberia (4262), Nigeria (20), Senegal (1), Serra Leone (3410), Spain (1), and USA (3); up to the end of 14 October. There have been approximately 4595 deaths.

There are five strains of the Ebola virus different with their virulence in humans [9] and fatality rates: Bundibugyo (30% mortality rate [49]), Ivory Coast (0% [25]), Reston, Sudan (50% case-fatality rate [41,44]) and Zaire (with mortality rates of 55% to 88% [5,47,55]), all named after their places of origin. Four of these five have caused disease in humans. While the Reston virus can not infect humans, no illnesses or deaths have been reported and all the strains can cause disease in animals [28,38].

Ebola can be caught from both humans, animals and fruit bats. It is transmitted through close contact with blood, secretions, or other bodily fluids. Infection has been documented through the handling of infected chimpanzees, gorillas, fruit bats, monkeys, forest antelope and porcupines found dead or ill in the rainforest.

When an infection does occur in humans, the virus can be spread in several ways to others. Ebola is spread through direct and/or indirect contact (through broken skin or mucous membranes in, for example, the eyes, nose, or mouth) with

(a) - blood or body fluids (including but not limited to urine, saliva, sweat, stool, vomits, breast milk, and semen) of a person who is sick with Ebola.

(b) - infected semen/breast milk of men/women: men who have recovered clinically from the illness can still spread the virus to their partner through their semen for up to 7 weeks after recovery. Similarly, women who recovered clinically can still transmit the disease to their children for weeks through breast-feeding.

(c) - objects (like used needles, bed linen and used syringes, soiled clothing) that have been contaminated with the virus. Actually, infection can also occur if broken skin or mucous membranes of a healthy person come into contact with environments that have become contaminated with an Ebola patient's infectious fluids such as soiled clothing, bed linen, or used needles and syringes [33,47,57,59]. Moreover, since, according to the works in [7,42,59], filoviruses (thus Ebola virus) can survive in liquids, plastic surfaces and on solid substrates (glasses, sanitary equipments) for 14 to 50 days.

(d) - infected animals and bats: in Africa, Ebola may be spread as a result of handling bush-meat (wild animals hunted for food) and contact with infected bats. There is no evidence that mosquitoes or other insects can transmit Ebola virus. Only mammals (for example, humans, bats, monkeys, and apes) have shown the ability to become infected with and spread Ebola virus. Ebola virus has also been spreading among wild nonhuman primates, apparently as a result of their contact with the unidentified reservoir host [4,29,33, 43,40]. This has contributed to a marked reduction in chimpanzee and gorilla populations and has also triggered human epidemics, presumably due to consumption of sick or dead

animals as a source of food [24,34]. The primary non-human reservoirs of Ebola are probably fruit bats [33,40].

(e) - cadavers during burials where mourners have direct contact with the deceased can also transmit the virus.

(f) - gloves, masks or protective goggles: healthcare workers have frequently been infected while treating Ebola patients. This has occurred through close contact without the use of gloves, masks or protective goggles. To date, nearly 180 health care workers have been infected, and more than 80 have died [14]. These latter transmission features [(c)-(f)] naturally raise the research question under investigation on which we shall focus.

Early on, the symptoms of EVD are non-specific. The disease is often characterized by the sudden onset of fever, feeling weak, muscle pains, headaches and a sore throat. This is followed by vomiting, diarrhea, rash, impaired kidney and liver function and, in some cases, internal and external bleeding. Symptoms can appear from 2 to 21 days after exposure. Some patients may go on to experience rashes, red eyes, hiccups, chest pains, difficulty in breathing and swallowing.

Standard treatment is limited to supportive therapy consisting of hydrating the patients, maintaining their oxygen status and blood pressure and treating them for any complicating infections. Once a patient recovers from Ebola, he/her is immune to the strain of the virus he/her contracted [47].

Responses to cases involves isolation and treatment of patients, contact tracing and monitoring each contact for 21 days (maximum incubation period) after exposure [21,47]. It is difficult to isolate and care for patients with EVD not because the disease is particularly infectious or the virus particularly hardy, but because a single lapse can be devastating: if a single case is missed, a single contact becomes ill and if isn't isolated, another chain of transmission can start [48]. There are three key preventive interventions.

The first is meticulous infection control in health care settings. The greatest risk of transmission is not from patients with diagnosed infection but from delayed detection and isolation. Since the early symptoms of EVD (fever, nausea, vomiting, diarrhea, and weakness) are nonspecific and common, patients may expose family caregivers, health care workers, and other patients before the infection is diagnosed. The second is educating and supporting the community to modify long-standing local funeral practices to prevent contact with body fluids of people who have died from EVD, at least temporarily until the outbreak is controlled. This key prevention strategy will close the second major route of propagation of the virus. This is a culturally sensitive issue that requires culturally appropriate outreach and education. The third is avoiding handling of bush meat (wild animals hunted for sustenance) and contact with bats (which may be the primary reservoir of Ebola virus) which may reduce the risk of initial introduction of Ebola virus into humans. Bush meat consumption could be reduced through socioeconomic development that increases access to affordable protein sources. Where bush meat consumption continues, safer slaughter and handling can be encouraged [47,53,56,57].

Since the onset of EVD in 1976, very few mathematic models [1,2,16,17,22,27,31,48] have been built and analyzed to help understanding the transmission and the dynamics of the disease. They all dealt only with human population, neglecting the effect of the environmental source of transmission. The aforementioned models did not incorporate the effect of the contaminated environment and the contamination of the environment by Ebola-infected individuals on the transmission dynamics of EVD in the communities (hence, they may have under-estimated EVD burden). More precisely, the work in [16], apart from providing a comprehensive review for the past Ebola models, have mentioned the influence of the environment on the transmission of EVD, even though, none all the past Ebola models reviewed there has incorporated that important feature. The purpose of the current study is to assess the role of the environment on the transmission dynamics of EVD in a human population. To achieve this objective, two new deterministic compartmental

models, which incorporate the above and other relevant epidemiological, demographic and biological features of EVD, are developed. The first model which we shall refer to as "full model" takes into account the environmental contamination. To allow comparison and assess the role of the environment, we develop a second model which can be regarded as a sub model of the full model and does not incorporate the environmental contamination. The specific goals are to determine the key factors that drive the disease transmission process and to propose effective and affordable strategies to minimize the spread of the disease. Our aim in this work is therefore to propose and analyze the proposed models for the dynamic of EVD in such a complex setting which take into consideration the known (direct) and suspected/probable (indirect environmental) contamination pathways. The incorporation of such unavoidable indirect environmental transmission route account for the assessment of the role of the environment in the spreading and the severity of EVD.

The models have been analyzed theoretically and numerically. From the theoretical point of view, we have established the following results.

(1) The disease-free equilibrium for the full model is GAS whenever the corresponding threshold quantity $\mathcal{R}_0^{env}$ is less than or equal to unity,
(2) In the case $\mathcal{R}_0^{env} > 1$, there exists a unique endemic equilibrium for the full model which is GAS.
(3) For the sub model without the environmental contamination, the disease-free equilibrium is GAS when the corresponding basic reproduction number $\mathcal{R}_0^h$ is less than or equal to unity.
(4) The said sub-model exhibits a unique endemic equilibrium, which is GAS whenever $\mathcal{R}_0^h > 1$.
(5) The two models are compared at endemic level and for both cases in items (2) and (4) above, the number of infected individuals obtained in the presence of the environmental transmission, is greater than the corresponding number of infected individuals in the absence of the environmental transmission.

As it is the case for most systems of differential equations that model real-life situations, the deterministic model designed in this paper can unfortunately not be solved explicitly by analytic techniques. It is therefore vital to perform numerical simulations through classical methods that aim at capturing the essential and/or expected properties of the continuous model. Thus, from the numerical point of view, we first carry out the sensitivity analysis of the model to identify the most influential parameters on the model output variables, that is the most robust estimations that are required and secondly apply the fourth Runge-Kutta method implemented in MatLab language, given its power to produce more precise approximated and faster convergent solutions in many applied areas.

The rest the paper is organized as follows. In Section 2, we formulate the models: the model with the environmental contamination (full model) and the sub model without the environmental contamination. The theoretical analysis of the full model is provided in Section 3. In Section 4, we give the complete analysis of the sub-model with only direct transmission (i.e., without the environmental contamination), and the role of the environmental contamination on the transmission of EVD is assessed theoretically and numerically. Section 5 presents the sensitivity analysis of the full model and the results of numerical simulations. Section 6 concludes the paper and provides some discussions that highlight few relevant perspectives.

2 Model formulation

Based on the infection modes displayed in the introduction part, we refer to the transmission routes (c) to (f) as the "*environment*". In fact, apart from the human-human contamination

modes involving direct contacts between infected and susceptible humans ((a) - (b)), there are the transmission routes (c) to (f) which are indirect and may involve the consumption of contaminated bush meat (animals hunted for food), manipulation and consumption of fruits bats, consumption of fruits contaminated by bats during deliverance (harvested in the rainforest for food during dry season when food is rare). To make our full model as simple as possible, we then encompass all these transmission modes in one class which we refer to as "*Environment*".

Therefore, our full model falls in the modeling framework for human diseases with free-living pathogens. It involves human individuals as host and the Ebola viruses in the environment as "reservoir" of pathogens [4,29,33,43,40]. We emphasize that the concentration of the Ebola viruses in the environment is not an epidemiological class: it is in fact an environmental compartment referred to as a "pool" of Ebola viruses [20] through which the human individuals can come into contact with and probably catch the infection.

The presence of the viruses in the environment account for the indirect transmission. This contaminated environment can be supplied by:

(i) the provision of contaminated Ebola-deceased animals, the manipulation consumption of infected fruit bats hunted by humans either for food or commercialization;
(ii) the contaminated fruits [26,33] harvested for food during food shortage in the dry seasons;
(iii) the shedding of viruses by infected/ Ebola-deceased human individuals through their bed linen, stool, urine, vomits or sweat [47,53,57]. This happens usually in health care centers or in family homes of infected and Ebola-deceased individuals.

2.1 The state variables

Here, we define the population variables and the epidemiological parameters used to develop our EVD transmission models. As mentioned above, the full model involves two populations, namely, the human population, the concentration of free living Ebola virus in the environment (which account for the indirect transmission).

2.1.1 Human population state variables

The total population of humans at time t, $N_h(t)$ is composed of four disjoint epidemiological classes, namely: susceptible human individuals to EVD $S_h(t)$ (i.e. who are completely free of the virus); exposed human individuals to EVD $E_h(t)$ (i.e. infected in latent stage); infectious humans individuals $I_h(t)$ (i.e. able to transmit EVD) and recovered humans individuals $R_h(t)$ (i.e. either clinically or completely). It is worth noting that, there is no specific treatment for EVD, but some patients recover after intensive supportive care by oral re-hydration with solutions containing electrolytes. Thus, the total human population at time t $N_h(t)$ is

$$N_h(t) = S_h(t) + E_h(t) + I_h(t) + R_h(t). \tag{2.1}$$

It is reported in [47,53] on the one hand that, the clinically recovered individuals still infect people during sexual intercourse. On the other hand that EVD-deceased individuals can still infect during burial ceremonies where their cadavers are manipulated by family members and mourners [47,53]. This latter feature is said to play the most important role in the disease transmission and persistence of EVD [20]. We are not going to use additional classes to account for these aspects, yet, we stress that the above mentioned facts will be incorporated in the incidence functions. Thus, it is suitable to model the transmission dynamics in the human population by a SEIR compartmental model.

2.1.2 Ebola virus concentration variable in the environment

As reported in [20,33,34,51,59], the indirect transmission through free living Ebola viruses in the environment occurs. Precisely, according to the works in [7,42], filoviruses (thus Ebola virus) can survive in liquids, plastic surfaces, and on solid substrates (glasses, sanitary equipments) for 14 to 50 days and remain viable. Moreover it is shown in [59] that there is evidence for environmental contamination, which may increase the risk of nosocomial transmission. Thus, we find it realistic to consider the concentration of the Ebola virus in the environment, with $V(t)$ being the concentration of any Ebola virus species (*Bundibugyo, Ivory-Coast, Reston, Sudan, Zaire*) harmful to humans, animals or bats.

2.2 Assumptions

The dynamics of EVD is governed by the following set of epidemiological hypotheses.

- (**H$_1$**) Infected individuals shed the Ebola viruses in the environment.
- (**H$_2$**) In almost all the EVD outbreaks in Africa, the case fatality rate is greater than or equal to 1/2. Thus, we assume $f \geq 1/2$.
- (**H$_3$**) Ebola-deceased individuals can continue to infect (during funerals).
- (**H$_4$**) Clinically recovered individuals still transmit the disease (through sexual intercourse or through breast-feeding).
- (**H$_5$**) The Ebola viruses in deceased individuals (the immune system defense is very poor or inexistent) is assumed to be more virulent than those in alive ones.
- (**H$_6$**) Long live immunity is assumed for recovered individuals. Indeed, the immunity induced by EVD infection is unknown, since it has never been reported that an individual have caught the infection for the second time.

2.3 The incidence functions and model equations

Based on the above assumptions, we derive the human-to-human force of infection λ_{hh}, the environment-to human force of infection λ_{hv} as well as the differential equations which describe the time evolution of the state variables under consideration.

2.3.1 Human-Human (human-to-human) force of infection: λ_{hh}

The high fatality rate of EVD lead to a big fear of the disease. Therefore, it is reasonable to assume that during the onset of the disease, people avoid crowded areas, for homogenous missing is harmful. This leads to a realistic assumption that the human-human force infection should be frequency-dependent (standard). Moreover, on the one hand, according to hypothesis (**H$_3$**), Ebola-deceased individuals can still contaminate during funeral practices if they are manipulated by mourners who enter into contact with their blood or any other bodily fluids [47,55]. On the other hand, clinically recovered men/women have Ebola viruses in their semen/breast milk up to seven (07) weeks after recovery [2,47,57]. Therefore, they can still infect other people via sexual intercourse. Thus, the human-to-human infection occurs as a result of three contributions:

1) Through an effective contact at rate β_{hh} with an infected human (I_h) who is still alive leading to the incidence function λ_{hI}, with

$$\lambda_{hI} = \frac{\beta_{hh} I_h}{N_h}. \tag{2.2}$$

2) Through an effective contact at rate $\xi_h \nu_h \gamma f \beta_{hh}$ with an EVD deceased individual yielding to the force of infection

$$\lambda_{hD} = \frac{\xi_h \nu_h \gamma f \beta_{hh} I_h}{N_h}, \tag{2.3}$$

where $\xi_h = 1/\tau_h$. The quantity γf is the fraction of infectious individuals who passed away due to EVD; ν_h is the virulence of Ebola viruses in the body of a EVD-deceased person and τ_h is the mean time that elapse after death before a cadaver is completely buried.

3) Via effective contact at rate $\beta_{hh}\theta_h(1-f)$ with a clinically recovered individual (R_h) yielding to the incidence function:

$$\lambda_{hR} = \frac{\theta_h \gamma (1-f) \beta_{hh} I_h}{N_h}, \quad \text{where} \quad \theta_h = 1/r_h. \tag{2.4}$$

The quantity $\gamma 1-f)$ is the fraction of infectious individuals who clinically recovered from the disease whereas r_h is the mean time that elapse before the complete clearance of Ebola viruses in the semen or breast milk of recovered individuals. Finally, the human-to-human force of infection is

$$\lambda_{hh} = \lambda_{hI} + \lambda_{hD} + \lambda_{hR} = \frac{\beta_{hh}}{N_h}\left(1 + \xi_h \nu_h \gamma f + \theta_h \gamma (1-f)\right) I_h. \tag{2.5}$$

2.3.2 Environment-Human (Environment-to-human-to-environment) force of infection: λ_{hv}

This transmission occurs indirectly. One way is through consumption of Ebola viruses in contaminated fruits by bats during competition for food in dry seasons, consumption of contaminated bush meat (animals and bats hunted for food) [33,40]. The other way is through contact with contaminated linen, urine (on soiled sanitary equipments) or stools of and infected person [47,53,56]. It is important to stress that humans, and some animals (non-human primates, apes, antelopes, monkeys, duikers) and fruit bats are mammals and can share some of the fruits as meal. This amounts in getting infection or consuming the Ebola viruses, with the Ebola viruses standing for the free living pathogens. Let β_{hv} be the effective ingestion rate of Ebola virus. Similar to [6,10,18], we assumed that an individual must consume at least the concentration (K) of Ebola virus equivalent to an amount that increases the possibility of being infected to about 50%. Thus, following the modeling framework for diseases transmitted by free living pathogen (Cholera, Typhoid fever, etc...), we use the Holling type II or Michaelis-Menten function dose response so that the force of infection is given by

$$\lambda_{hv} = \frac{\beta_{hv} V}{K + V}. \tag{2.6}$$

Note however, since the Ebola virus is highly infectious, the minimum infection dose K can be very low. Thus λ_{hv} can be modeled using mass action incidence (i.e. $\lambda_{hv} = \beta_{hv} V$).

In summary, the overall force of infection in human's population denoted by λ_h is

$$\lambda_h = \lambda_{hh} + \lambda_{hv} = \frac{\beta_{hh}\left(I_h + \xi_h \nu_h \gamma f I_h + \theta_h \gamma (1-f) I_h\right)}{N_h} + \frac{\beta_{hv} V}{K + V}. \tag{2.7}$$

The susceptible population S_h is replenished by a constant recruitment at rate Λ_h into the community. These latter individuals may acquire infection following the force of infection λ_h, and die naturally at rate μ_h. It is assumed that the exposed individuals E_h do not transmit the disease, maybe as a result of perfect implementation of contact tracing and isolation. Those who recovered from EVD will not return in the susceptible class, maybe as a result of their behavior adjustment due to the fear of the disease. The exposed class E_h is generated

by the susceptible individuals who became infected at rate λ_h. This latter population is decreased when they become infectious at rate ω and move to the infectious class I_h, or when they die naturally at rate μ_h. The infectious compartment I_h diminish when they recover (after supportive care) at rate γ and therefore increase the recovered class R_h. Both the infectious and the recovered population die at rate μ_h as well.

The concentration V of Ebola viruses in the environment is modeled following [10,18, 50]. We apply the framework modeling of the free living pathogen similar to diseases like, cholera, typhoid, or yellow fever. Thus, the dynamics of the concentration of the free living Ebola viruses is given by

$$\frac{dV}{dt} = \alpha_h I_h - \mu_v V, \tag{2.8}$$

where α_h is the sledding rate of Ebola viruses in the environment by infected individuals.

A schematic model flowchart is depicted in Fig. 1. The corresponding system of differential equations is

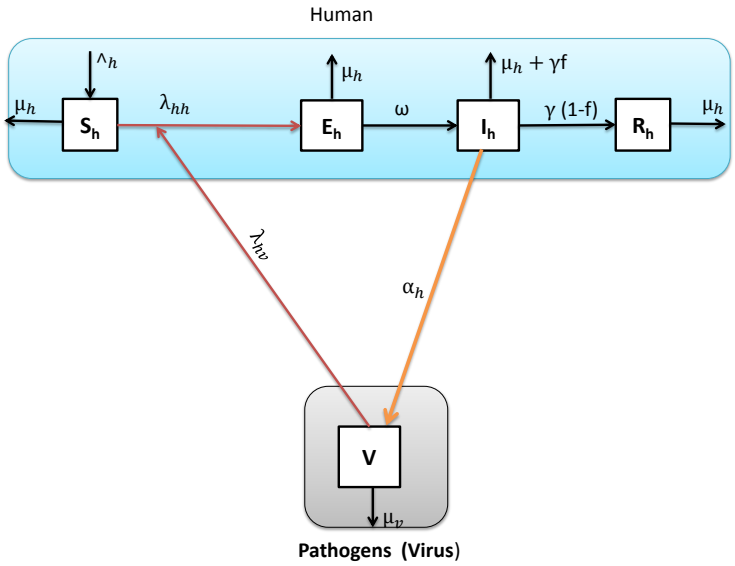

Fig. 1 Ebola Virus Disease transmission flow diagram

$$\begin{cases} \dfrac{dS_h}{dt} = \Lambda_h - \dfrac{\beta_{hh}\Phi_h S_h I_h}{N_h} - \dfrac{\beta_{hv} S_h V}{K+V} - \mu_h S_h, \\ \dfrac{dE_h}{dt} = \dfrac{\beta_{hh}\Phi_h S_h I_h}{N_h} + \dfrac{\beta_{hv} S_h V}{K+V} - (\mu_h + \omega) E_h, \\ \dfrac{dI_h}{dt} = \omega E_h - (\mu_h + \gamma) I_h, \\ \dfrac{dR_h}{dt} = \gamma(1-f) I_h - \mu_h R_h, \\ \dfrac{dV}{dt} = \alpha_h I_h - \mu_v V, \end{cases} \tag{2.9}$$

where $\Phi_h = 1 + \xi_h \nu_h \gamma f + \theta_h \gamma (1-f)$.

Table 1 recapitulates the relevant parameters used to develop the model. Throughout this paper, we shall refer to system (2.9) as the full model. Note that he associated model

Parameter	Biological interpretation
Λ_h	Recruitment rate of susceptible individuals.
μ_h	Natural dead rate of all individuals.
ν_h	Virulence of Ebola viruses in the corpse of the deceased individuals.
τ_h	Mean burial time.
$\xi_h = 1/\tau_h$	Modification parameter of infectiousness due to EVD-deceased individuals.
ω	Incubation period rate of infected individuals.
γ	Removal rate from infectious class due to disease induced death or by recovery.
α_h	Shedding rate of Ebola viruses in the environment by infected individuals.
r_h	Mean clearance time of Ebola viruses in the recovered individuals
$\theta_h = 1/r_h$	Modification parameter of contact rate of recovered humans due to the presence of Ebola viruses in the semen/breast milk of a recovered man/woman.
f	Proportion of EVD-deceased individuals: case fatality.
K	Virus 50 % infectious dose, sufficient to cause EVD infection.
β_{hh}	Effective contact rate between susceptible and infected individuals .
β_{hv}	Effective contact rate between susceptible individuals and Ebola viruses.
μ_v	Decay rate of Ebola viruses in the environment.

Table 1 Model parameters and their biological/epidemiological interpretations.

without environmental contamination which will be analyzed in details in Subsection 4.1 is obtained by neglecting the indirect contamination through contact with the contaminated environment and is modeled by

$$\begin{cases} \dfrac{dS_h}{dt} = \Lambda_h - \dfrac{\beta_{hh}\Phi_h S_h I_h}{N_h} - \mu_h S_h, \\ \dfrac{dE_h}{dt} = \dfrac{\beta_{hh}\Phi_h S_h I_h}{N_h} - (\mu_h + \omega) E_h, \\ \dfrac{dI_h}{dt} = \omega E_h - (\mu_h + \gamma) I_h, \\ \dfrac{dR_h}{dt} = \gamma(1-f) I_h - \mu_h R_h. \end{cases} \tag{2.10}$$

We shall study in details this model (2.10) later in Subsection 4.1.

It is important to compared the model (2.9) with few deterministic existing models. The proposed model (2.9) extends the works in [1,2,17,22,31,32,39,51] by:

1. considering the indirect transmission via the environment. None of the above mentioned works have considered such a aspect while modeling EVD. They concentrated only on the human population, without modeling the environmental source of the disease (i.e. from where the disease triggers and enters the human population). Indeed, the incorporation of the environmental contamination feature is motivated by the fact that, for almost all the EVD outbreaks, it has been reported the index case (first patient) got the infection from the environment (after manipulation for food near the rain forests).
2. including the contamination through recovered individuals which is not the case in none of the works mentioned above.
3. incorporating the demographic dynamics.
4. considering infection through contact with deceased humans (during funerals). Moreover, contrary to [39,51] where an epidemiological class for EVD-deceased individuals was explicitly considered, our model, for the sake of simplicity do not consider dead individuals as an explicit compartment. However, these latter individuals are considered to be infectious until they are completely buried. A part from [31,39], none of the mentioned works have considered such an important characteristic.
5. modeling the dead-mediated and the clinically recovered-mediated transmissions using fractions of infectious (I_h) individuals, whereas in [31] the authors explicitly incorporated the death in the force of infection.

6. assuming the virulence of the Ebola viruses in EVD-deceased individuals. Actually, the viruses inside the body of EVD-deceased individuals are supposed to be more virulent than those in the alive infected individuals.

3 Mathematical analysis of the full model

3.1 Positivity and boundedness of solutions

For the EVD transmission model (2.9) to be epidemiological meaningful, it is important to prove that all the states variables are non-negative for all time. In other words, solutions of system (2.9) with non-negative initial data will remain non-negative for all $t > 0$.

Theorem 3.1 *If the initial data* $(S_h(0), E_h(0), I_h(0), R_h(0), V(0)) \geq 0$, *then the solutions* $(S_h(t), E_h(t), I_h(t), R_h(t), V(t))$ *of system (2.9) are non-negative for all* $t > 0$, *and the positive orthant* $\mathbb{R}^5_+$ *is positively invariant with respect to the flow of system (2.9).*

Furthermore, for initial conditions such that

$$N_h(0) \leq \frac{\Lambda_h}{\mu_h}, \quad V(0) \leq \frac{\alpha_h \Lambda_h}{\mu_h \mu_v},$$

we have

$$N_h(t) \leq \frac{\Lambda_h}{\mu_h}, \quad V(t) \leq \frac{\alpha_h \Lambda_h}{\mu_h \mu_v}, \ \forall t \geq 0.$$

Proof: Suppose $S_h(0) \geq 0$, then from the first equation of system (2.9) and an argument on continuous functions, $S_h(t)$ remains non-negative on a small interval in the right hand side of $t_0 = 0$. Therefore, there exists $t_m = \sup\{t \geq 0 : \ S_h(t) \geq 0\}$. Obviously $t_m \geq 0$ by definition. To show that $S_h(t) \geq 0$ for all $t \geq 0$, we only need to prove that $S_h(t_m) > 0$. It follows from the first equation of system (2.9) that

$$\frac{dS(t)}{dt} = \Lambda_h - (\lambda_h(t) + \mu_h)S_h\,, \quad \text{where } \lambda_h \quad \text{is given by Eq. (2.7)},$$

which can be rewritten as

$$\frac{d}{dt}\left\{S_h(t)\exp\left(\int_0^t (\lambda_h(p) + \mu_h)dp\right)\right\} = \Lambda_h \exp\left(\int_0^t (\lambda_h(p) + \mu_h)dp\right).$$

Hence, integrating this last relation with respect to t from 0 to t_m, we have

$$S_h(t_m)\exp\left(\int_0^{t_m} (\lambda_h(p) + \mu_h)dp\right)dt - S_h(0) = \int_0^{t_m} \Lambda_h \exp\left(\int_0^t (\lambda_h(p) + \mu_h)dp\right)dt$$

so that the multiplication of both side by $\exp\left(\int_0^{t_m} -(\lambda_h(p) + \mu_h)dp\right)$ yields

$$S_h(t_m) = \left[S_h(0) + \int_0^{t_m} \Lambda_h \exp\left(\int_0^t (\lambda_h(p) + \mu_h)dp\right)dt\right] \times \exp\left(\int_0^{t_m} -(\lambda_h(p) + \mu_h)dp\right)$$

From this, we deduce that $S_h(t_m) > 0$, and thus $S_h(t) > 0$ for all $t > 0$.
The same arguments can be used to prove that $E_h(t), I_h(t), R_h(t), V(t) \geq 0$ for all $t > 0$.

Furthermore,

$$\frac{dN_h}{dt} = \Lambda_h - \mu_h N_h - \gamma f I_h \leq \Lambda_h - \mu_h N_h.$$

Thus, by Gronwall inequality, we have

$N_h(t) \leq N_h(0)e^{-\mu_h t} + \frac{\Lambda_h}{\mu_h}(1 - e^{-\mu_h t})$ and then $N_h(t) \leq \frac{\Lambda_h}{\mu_h}$, $\forall t \geq 0$ whenever $N_h(0) \leq \frac{\Lambda_h}{\mu_h}$.

Finally, using the fact that $I_h \leq N_h$ and the Gronwall inequality, lead us to

$$V(t) \leq \frac{\alpha_h \Lambda_h}{\mu_h \mu_v}, \ \ \forall t \geq 0 \ \text{ whenever } \ V(0) \leq \frac{\alpha_h \Lambda_h}{\mu_h \mu_v}.$$

This completes the proof.

□

Combining Theorem 3.1 together with the trivial existence of a unique local solution for the model (2.9), we have established the following theorem which ensures the mathematical and biological well-posedness of system (2.9).

Theorem 3.2 *The model (2.9) is a dynamical system in the biological feasible compact set*

$$\Gamma_h = \left\{ (S_h, E_h, I_h, R_h, V) \in \mathbb{R}^5_+ : N_h \leq \frac{\Lambda_h}{\mu_h}, \ \ V(t) \leq \frac{\alpha_h \Lambda_h}{\mu_h \mu_v} \right\}.$$

3.2 The disease-free equilibrium and its stability

The disease free equilibrium (DFE) of the model is obviously

$$P_h^0 = \left(S_h^0, 0, 0, 0, 0 \right), \ \text{ with } \ S_h^0 = \frac{\Lambda_h}{\mu_h}.$$

We use the next generation method developed in [3,6,19,52] to compute the basic reproduction number. The vectors $\mathcal{F} = (\lambda_h S_h, 0, 0, 0)^T$ and $\mathcal{W} = ((\mu_h + \omega) E_h, -\omega E_h + (\mu_h + \gamma) I_h, -\gamma(1-f) I_h + \mu_h R_h, -\alpha_h I_h + \mu_v V)^T$ represent the new infection terms and the remaining transfer terms, respectively. Their Jacobian matrices evaluated at the DFE are given by

$$F = \begin{pmatrix} 0 & \beta_{hh} \Phi_h & 0 & \dfrac{\beta_{hv} \Lambda_h}{\mu_h K} \\ 0 & 0 & 0 & 0 \\ 0 & 0 & 0 & 0 \\ 0 & 0 & 0 & 0 \end{pmatrix} \quad \text{and} \quad W = \begin{pmatrix} (\mu_h + \omega) & 0 & 0 & 0 \\ -\omega & (\mu_h + \gamma) & 0 & 0 \\ 0 & -\gamma(1-f) & \mu_h & 0 \\ 0 & -\alpha_h & 0 & \mu_v \end{pmatrix}.$$

Simple calculations show that the basic reproduction number $\mathcal{R}_0^{env}$ is given by

$$\mathcal{R}_0^{env} = \frac{\beta_{hh} \Phi_h \omega}{(\mu_h + \omega)(\mu_h + \gamma)} + \frac{\alpha_h \beta_{hv} \Lambda_h \omega}{K \mu_h \mu_v (\mu_h + \omega)(\mu_h + \gamma)}. \tag{3.1}$$

Remark 3.3 *A comparison of the basic reproduction number $\mathcal{R}_0^{env}$ defined in Eq. (3.1) with those for the existing models (provided one relaxes some of the hypothesis stated for the modeling) allows the estimation of the transmissive power of the disease.*

The relevance of the reproduction number is due to the following result established in [52].

Lemma 3.4 *The DFE P_h^0 of system (2.9) is locally asymptotically stable (LAS) if $\mathcal{R}_0^{env} < 1$, and unstable if $\mathcal{R}_0^{env} > 1$.*

The epidemiological implication of Lemma 3.4 is that the Ebola virus disease can be eliminated from the community when $\mathcal{R}_0^{env} < 1$ if the initial sizes of the different sub-populations of the model are in the basin of attraction of the DFE P_h^0. For a better control on the disease, the GAS of the DFE is needed. Actually, enlarging the basin of attraction of P_h^0 to be the entire Γ_h is, for the model under consideration a more challenging task. We have the following result.

Theorem 3.5 *The DFE P_h^0 of the system (2.9) is GAS if $\mathcal{R}_0^{env} < 1$ in Γ_h.*

Proof: Let $x = (E_h, I_h, R_h, V)$ and $y = S_h$, be the infected and uninfected states, respectively. The system (2.9) can be re-written as

$$\begin{cases} \dfrac{dx}{dt} = (F - W)\, x - f(x, y) \\ \dfrac{dy}{dt} = g(x, y), \end{cases} \tag{3.2}$$

where F and W are given above,

$$f(x,y) = \begin{pmatrix} (N_h - S_h)\dfrac{\beta_{hh}\Phi_h I_h}{N_h} + \beta_{hv} V\left(\dfrac{\Lambda_h}{\mu_h K} - \dfrac{S_h}{K+V}\right) \\ 0 \\ 0 \\ 0 \end{pmatrix}; \quad g(x,y) = \Lambda_h - \lambda_h S_h - \mu_h S_h.$$

It is straightforward that $f(x, y) \geq 0$ for all $(x, y) \in \Gamma_h$. Therefore, $dx/dt \leq (F - W)\, x$, we then consider the following auxiliary linear subsystem from system(3.2):

$$\frac{d\widehat{x}}{dt} = (F - W)\,\widehat{x} \tag{3.3}$$

From Theorem 2 in [52], we have $\mathcal{R}_0^{env} < 1 \iff \sigma(F - W) < 0$, where $\sigma(M)$ is the stability modulus of the matrix M. Thus, when $\mathcal{R}_0^{env} < 1$, all the eigenvalues of $F-W$ have negative real parts. Thus, the non-negative solutions of (3.3) are such that $\lim_{t\to+\infty} \widehat{x} = 0$, or equivalently $\lim_{t\to+\infty} \widehat{E_h} = \lim_{t\to+\infty} \widehat{I_h} = \lim_{t\to+\infty} \widehat{V} = 0$. By the standard comparison principle [30,45] and the non-negativity of x, the non-negative solutions of (2.9) satisfy $\lim_{t\to+\infty} E_h = 0$, $\lim_{t\to+\infty} I_h = \lim_{t\to+\infty} V = 0$. Therefore, since $\lim_{t\to+\infty} x = 0$, system (2.9) is an asymptotically autonomous system [12] (Theorem 2.5) with the limit system as follows

$$\frac{d\widetilde{S_h}}{dt} = \Lambda_h - \mu_h \widetilde{S_h}. \tag{3.4}$$

It is obvious that the affine system (3.4) has a unique equilibrium giving by S_h^0 which is GAS. This completes the proof.

□

Remark 3.6 *An alternative proof of Theorem 3.5 can be done using the Lyapunov techniques. Indeed, it suffices to use the following Lyapunov function:*

$$L_0\,(E_h, I_h, R_h, V) = \left[\frac{b\omega}{B} + \frac{d\omega\alpha_h}{\mu_v B}\right] E_h + \left[\frac{b\mu_h + \gamma}{B} + \frac{d\alpha_h}{\mu_v\,(\mu_h + \gamma)}\right] I_h + \frac{d}{\mu_v} V, \tag{3.5}$$

where

$$b = \beta_{hh}\Phi_h, \quad d = \frac{\beta_{hv}\Lambda_h}{K\mu_h} \qquad \text{and} \quad B = (\mu_h + \gamma)\,(\mu_h + \omega)\,.$$

Since $S_h^0 = \Lambda_h/\mu_h$, the time derivative of L_0 is

$$\begin{aligned} \dot{L}_0 &= \left[\left(\frac{b\omega}{B} + \frac{d\omega\alpha_h}{\mu_v B}\right)\frac{S_h}{N_h} - 1\right] bI_h + \left[\left(\frac{b\omega}{B} + \frac{d\omega\alpha_h}{\mu_v B}\right)\frac{S_h K}{S_h^0(K+V)} - 1\right] dV, \\ &= \left[\mathcal{R}_0^{env}\frac{S_h}{N_h} - 1\right] bI_h + \left[\mathcal{R}_0^{env}\frac{S_h K}{S_h^0(K+V)} - 1\right] dV, \\ &= \left[\left(\mathcal{R}_0^{env} - 1\right) S_h - (E_h + R_h + I_h)\right]\frac{bI_h}{N_h} \\ &\quad + \left[\left(\mathcal{R}_0^{env} - 1\right) K\mu_h S_h^0 S_h - K\Lambda_h\left(S_h^0 - S_h\right) - K\Lambda_h S_h^0 V\right]\frac{dV}{S_h^0\Lambda_h(K+V)}. \end{aligned} \tag{3.6}$$

Thus, if $\mathcal{R}_0^{env} \leq 1$, $\dot{L}_0 \leq 0$ *in* Γ_h. *Then, LaSalle's Invariance Principle applied to the Lyapunov function* L_0 *allows to extend the GAS of the disease-free equilibrium to the case where* $\mathcal{R}_0^{env} = 1$. *In summary,* P_h^0 *is GAS whenever* $\mathcal{R}_0^{env} \leq 1$.

3.3 The endemic equilibrium and its stability

Herein, we compute the endemic equilibrium of system (2.9) and investigate its stability.

Let $P_h^* = (S_h^*, E_h^*, I_h^*, R_h^*, V^*)^T$ be any endemic equilibrium of system (2.9) where the components $S_h^*, E_h^*, I_h^*, R_h^*$ and V^* are the solutions of the following system of equations:

$$\begin{cases} \Lambda_h - \lambda_h^* S_h^* - \mu_h S_h^* = 0 \\ \lambda_h^* S_h^* - (\mu_h + \omega) E_h^* = 0 \\ \omega E_h^* - (\mu_h + \gamma) I_h^* = 0 \\ \gamma(1-f) I_h^* - \mu_h R_h^* = 0 \\ \alpha_h I_h^* - \mu_v V^* = 0, \end{cases} \tag{3.7}$$

where

$$\lambda_h^* = \frac{\beta_{hh} \Phi_h I_h^*}{N_h^*} + \frac{\beta_{hv} V^*}{K + V^*}. \tag{3.8}$$

From (3.7), $S_h^*, E_h^*, I_h^*, R_h^*, V^*$ and $N_h^* = S_h^* + E_h^* + I_h^* + R_h^*$ can be expressed in term of λ_h^* as follows:

$$\begin{cases} S_h^* = \dfrac{\Lambda_h}{\lambda_h^* + \mu_h}, \quad E_h^* = \dfrac{\lambda_h^* \Lambda_h}{(\lambda_h^* + \mu_h)(\mu_h + \omega)}, \quad I_h^* = \dfrac{\lambda_h^* \Lambda_h \omega}{(\lambda_h^* + \mu_h)(\mu_h + \omega)(\mu_h + \gamma)}, \\ R_h^* = \dfrac{\lambda_h^* \Lambda_h \omega \gamma (1-f)}{\mu_h (\lambda_h^* + \mu_h)(\mu_h + \omega)(\mu_h + \gamma)}, \quad V_h^* = \dfrac{\lambda_h^* \Lambda_h \alpha_h \omega}{\mu_v (\lambda_h^* + \mu_h)(\mu_h + \omega)(\mu_h + \gamma)}, \\ N_h^* = \dfrac{\Lambda_h \left[(\lambda_h^* + \mu_h)(\mu_h + \omega)(\mu_h + \gamma) - \omega \gamma f \lambda_h^* \right]}{\mu_h (\lambda_h^* + \mu_h)(\mu_h + \omega)(\mu_h + \gamma)}. \end{cases} \tag{3.9}$$

Substituting Eq. (3.9) into (3.8), the non-zero equilibrium of model (2.9) satisfy the following quadratic equation in λ_h^*:

$$p\,(\lambda_h^*)^2 + q\,\lambda_h^* - r = 0, \tag{3.10}$$

where

$$\begin{cases} p = (\omega \alpha_h \Lambda_h + \mu_v K B)\left[\mu_h (\mu_h + \omega + \gamma) + \omega \gamma (1-f)\right], \\ q = K \mu_h \mu_v B (B - \omega \gamma f) + \beta_{hv} \Lambda_h \alpha_h \omega (\omega \gamma f + \mu_h B) + \mu_h B \left(1 - \mathcal{R}_0^{env}\right)(\Lambda_h \alpha_h \omega + K \mu_v B), \\ r = \beta_{hh} A B K \omega \mu_v \mu_h + \beta_{hv} \alpha_h \omega \mu_h \Lambda_h B - \mu_h^2 \mu_v K B^2 = \mu_h^2 \mu_v K B^2 \left[\mathcal{R}_0^{env} - 1\right]. \end{cases} \tag{3.11}$$

with

$$A = \mu_h \Phi_h = \mu_h (1 + \xi_h \nu_h \gamma f + \theta_h \gamma (1-f)) \qquad \text{and} \qquad B = (\mu_h + \omega)(\mu_h + \gamma).$$

Note that $p > 0$ and $q > 0$ whenever $\mathcal{R}_0^{env} \leq 1$. Further $r > 0$ whenever $\mathcal{R}_0^{env} > 1$. Thus, by applying the Descartes rule of signs to the quadratic equation (3.10), the following result is established.

Theorem 3.7 *For system (2.9), the following statements hold.*

- *if* $\mathcal{R}_0^{env} > 1$, *there exists an unique endemic equilibrium giving by (3.9) where* λ_h^* *is the solution of (3.10).*
- *if* $\mathcal{R}_0^{env} \leq 1$, *there is no endemic equilibrium and the only steady state is the disease-free equilibrium.*

Actually, the explicit value of $\lambda_h^* > 0$, which is the unique positive solution of (3.10) is given by

$$\lambda_h^* = \frac{-q + \sqrt{q^2 + 4pr}}{2} \tag{3.12}$$

and the components of P_h^* are obtained by substituting this positive root of (3.10) into the steady-states expressions in (3.7).

Now, we investigate the stability of the unique endemic equilibrium P_h^*. We have obtained the following result.

Theorem 3.8 *If $\mathcal{R}_0^{env} > 1$, then system (2.9) undergoes the trans-critical bifurcation with $\mathcal{R}_0^{env} = 1$ being the bifurcation parameter. Moreover, the unique endemic equilibrium defined in Eqs. (3.9)-(3.12) is LAS.*

The proof of this theorem used the Center Manifold Theory as proposed in [13,11] and is given in the Appendix.

4 Impact of the environmental contamination on the transmission of EVD

In this section, we assess the role of the environmental contamination on the transmission of EVD. For this assessment to happen, we begin by analyzing system (2.9) without the indirect environmental contamination.

4.1 Analysis of the sub-model without environmental contamination

We recall that, in the absence of the environmental contamination (i.e., $\beta_{hv} = 0$), system (2.9) reduces to system (2.10), which we repeat here for convenience.

$$\begin{cases} \dfrac{dS_h}{dt} &= \Lambda_h - \dfrac{\beta_{hh}\Phi_h S_h I_h}{N_h} - \mu_h S_h, \\ \dfrac{dE_h}{dt} &= \dfrac{\beta_{hh}\Phi_h S_h I_h}{N_h} - (\mu_h + \omega) E_h, \\ \dfrac{dI_h}{dt} &= \omega E_h - (\mu_h + \gamma) I_h, \\ \dfrac{dR_h}{dt} &= \gamma(1-f) I_h - \mu_h R_h, \\ \dfrac{dV}{dt} &= \alpha_h I_h - \mu_v V. \end{cases} \tag{4.1}$$

The system (4.1) is mathematically and epidemiological well posed in the feasible region Γ_h. Also, system (4.1) is a dynamical system in Γ_h. The corresponding disease-free equilibrium X_h^0 is

$$X_h^0 = \left(\frac{\Lambda_h}{\mu_h}, 0, 0, 0, 0\right).$$

Without the environmental transmission (i.e. $\beta_{hv} = 0$), the basic reproduction number (3.1) becomes

$$\mathcal{R}_0^h = \frac{\beta_{hh}\Phi_h\omega}{(\mu_h + \omega)(\mu_h + \gamma)}. \tag{4.2}$$

We emphasize this latter the basic reproduction number $\mathcal{R}_0^h$ and the former $\mathcal{R}_0^{env}$ will be used to compare our models at the early stage of the disease and thus numerically assess the impact of the environmental contamination.

The existence of the unique endemic equilibrium point

$$\overline{X}_h = \left(\overline{S}_h, \overline{X}_h, \overline{I}_h, \overline{R}_h, \overline{V}\right),$$

is subjected to the human-human basic reproduction number $\mathcal{R}_0^h$ in Eq. (4.2) being larger than the unity. A simple calculation proves that

$$\begin{cases} \overline{S}_h &= \dfrac{\Lambda_h\left[\mu_h\left(\mu_h+\omega+\gamma\right)+\gamma\omega(1-f)\right]}{\mu_h\left[B\left(\mathcal{R}_0^h-1\right)+\mu_h\left(\mu_h+\omega+\gamma\right)+\gamma\omega(1-f)\right]}, \\ \overline{E}_h &= \dfrac{\left(\mu_h+\gamma\right)\Lambda_h\left(\mathcal{R}_0^h-1\right)}{B\left(\mathcal{R}_0^h-1\right)+\mu_h\left(\mu_h+\omega+\gamma\right)+\gamma\omega(1-f)}, \\ \overline{I}_h &= \dfrac{\omega\Lambda_h\left(\mathcal{R}_0^h-1\right)}{B\left(\mathcal{R}_0^h-1\right)+\mu_h\left(\mu_h+\omega+\gamma\right)+\gamma\omega(1-f)}, \\ \overline{R}_h &= \dfrac{\gamma(1-f)\omega\Lambda_h\left(\mathcal{R}_0^h-1\right)}{\mu_h\left[B\left(\mathcal{R}_0^h-1\right)+\mu_h\left(\mu_h+\omega+\gamma\right)+\gamma\omega(1-f)\right]}, \\ \overline{V} &= \dfrac{\omega\alpha_h\Lambda_h\left(\mathcal{R}_0^h-1\right)}{\mu_v B\left(\mathcal{R}_0^h-1\right)+\mu_h\left(\mu_h+\omega+\gamma\right)+\gamma\omega(1-f)}. \end{cases} \tag{4.3}$$

where

$$\overline{\lambda}_h = \frac{\mu_h B\left(\mathcal{R}_0^h-1\right)}{B-\omega\gamma f}. \tag{4.4}$$

The global stability analysis of model (4.1) is completely described by the following result.

Theorem 4.1 *The following statements are true:*

(1) The disease-free equilibrium point X_h^0 is GAS when $\mathcal{R}_0^h \leq 1$ and unstable if $\mathcal{R}_0^h > 1$.
(2) There is a unique endemic equilibrium point $\overline{X}_h$ which is GAS whenever $\mathcal{R}_0^h > 1$.

Proof: The first item is established using the Lyapunov function:

$$L_h = L_h\left(S_h, E_h, I_h, R_h, V\right) = \frac{\omega}{B_h}E_h + \frac{1}{\mu_h+\gamma}I_h. \tag{4.5}$$

The Lie derivative of L_h with respect to the vector field given by the right hand side of (4.1) is

$$\dot{L}_h = \left[\frac{\beta_{hh}\Phi_h\omega S_h}{B_h N_h} - 1\right]I_h = -\left[\left(1-\mathcal{R}_0^h\right)S_h + E_h + I_h + R_h\right]\frac{I_h}{N_h}. \tag{4.6}$$

Thus, $\dot{L}_h \leq 0$ in Γ_h, and $\dot{L}_h = 0$ if and only if $I_h = 0$ or $\mathcal{R}_0^h = 1$ and $E_h + I_h + R_h = 0$. In both cases, it is easy to check that the largest invariant set in $M_h = \left\{(S_h, E_h, I_h, R_h) \in \Gamma_h / \ \dot{L}_h = 0\right\}$ is the disease-free equilibrium point P_h^0. Indeed, suppose $I_h = 0$, then replacing it in the first, second and fourth equations of (4.1) and solve give $S_h(t) = \Lambda_h/\mu_h + \left[S_h(0) - \Lambda_h/\mu_h\right]e^{-\mu_h t}$, $E_h(t) = E_h(0)e^{-(\mu_h+\gamma)t}$ and $R_h(t) = R_h(0)e^{-\mu_h t}$. Similarly, as $t \to \infty$, $V(t) \to 0$. Thus, as $t \to \infty$, $S_h(t) \to \Lambda_h/\mu_h$, and $(E_h(t), E_h(t)) \to (0,0)$. Hence $M_h = \left\{P_h^0\right\}$. The GAS of P_h^0 follows by LaSalle's Invariance Principle. For the proof of the GAS of $\overline{X}_h$ in the second item, we refer the interested reader to [35,58] where the result is obtained by using the geometrical approach [36]. This concludes the proof.

□

4.2 Comparison of systems (2.9) and (4.1) at early stage and at endemic level.

The objective of this section is to compare the dynamics of EVD described by only direct human-human transmission (cf. Section 4.1) with the the dynamics of EVD in the case of both direct and indirect environment-to-human-to-environment transmission (cf. Section 3). Practically, this shall be done at two levels of the outbreak. First at early stage of the disease by simply comparing the respective basic reproduction numbers. Secondly at endemic level by quantitatively comparing the infectious components I_h^* and $\bar{I}_h$ of the corresponding endemic equilibria. Should these comparisons be possible, they allow to easily assess the impact of the environment compartment in the transmission of EVD.

The first comparison at early stage of the disease is straightforward since

$$\mathcal{R}_0^{env} > \mathcal{R}_0^h. \tag{4.7}$$

For the second comparison of the fate of the disease at the endemic level, the simplest way to tackle it analytically is to study the variations of $I_h^* = I_h^*(\beta_{hv})$ as a function of the effective contact rate $\beta_{hv} \geq 0$ with the environment, as well as the variations of $I_h^* = I_h^*(\alpha_h)$ with respect to the shedding rate $\alpha_h \geq 0$.

Remind that

$$I_h^* = I_h^*(\beta_{hv}) = \frac{\lambda_h^*(\beta_{hv})\Lambda_h\omega}{(\lambda_h^*(\beta_{hv}) + \mu_h)(\mu_h + \omega)(\mu_h + \gamma)},$$

where

$$\lambda_h^* = \lambda_h^*(\beta_{hv}) = \frac{-q(\beta_{hv}) + \sqrt{q^2(\beta_{hv}) + 4pr(\beta_{hv})}}{2p}.$$

Note that when there no contamination via the environment, $\beta_{hv} = 0 = K$. Thus,

$p(0) = p(K = 0) = \Lambda_h\alpha_h\omega\left(B - \omega\gamma f\right)$, $\quad r(0) = r(\beta_{hv} = 0) = 0$ and $q(0) = q(\beta_{hv} = 0) = \Lambda_h\alpha_h\omega\left(\mu_h B - \beta_{hh}\omega A\right)$.

In this case, the only solution of Eq. (3.10) is

$$\lambda_h^*(0) = \lambda_h^*(\beta_{hv} = 0) = \frac{-q(0)}{p(0)} = \frac{\beta_{hh}\omega A - \mu_h B}{B - \omega\gamma f} = \frac{\mu_h B\left(\mathcal{R}_0^h - 1\right)}{B - \omega\gamma f}.$$

It clearly appears that $\lambda_h^*(0)$ is equal to $\overline{\lambda}_h$ and consequently $I_h^*(0) = I_h^*(\beta_{hv} = 0) = \bar{I}_h$.

Now, from Eq. (3.12), the partial derivative of I_h^* with respect to β_{hv} satisfies

$$\frac{\partial \bar{I}_h}{\partial \beta_{hv}} = \frac{\omega\alpha_h\Lambda_h\left(B - \omega\gamma f\right)\left(\Sigma_1 - \Delta\right)}{2p\Delta}, \tag{4.8}$$

where

$$\Sigma_1 = \omega\alpha_h\Lambda_h\mu_h B + K\mu_h\mu_v B\omega\gamma f + \beta_{hh}\omega A\left(\mu_v K B + \omega\alpha_h\Lambda_h\right) + \beta_{hv}\omega\alpha_h\Lambda_h\left(B - \omega\gamma f\right),$$
$$\Delta = \Delta(\beta_{hv}) = \sqrt{q^2 + 4pr}.$$

The right hand side of Eq. (4.8) has the same sign as $\Sigma_1^2 - \Delta^2$. Direct calculations show that

$$\begin{aligned}
\Sigma_1^2 - \Delta^2 &= \Sigma_1^2 - q^2 - 4pr, \\
&= 4\omega^3\alpha_h^2\Lambda_h^2\mu_h B\beta_{hh}A + 4K^2\mu_h^2\mu_v^2B^3\omega\gamma f - 4K\mu_h^2\mu_v B^3\omega\alpha_h\Lambda_h \\
&\quad +4K^2\mu_h\mu_v^2B^3\beta_{hh}\omega A - 4\omega^3\alpha_h^2\Lambda_h^2\mu_h B\beta_{hv}\gamma f - 4K^2\mu_h^2\mu_v^2B^4 + 4\omega^2\alpha_h^2\Lambda_h^2\mu_h B^2\beta_{hv} \\
&\quad +4\omega^2\alpha_h\Lambda_h\mu_h^2B^2K\mu_v\gamma f + 8\omega^2\alpha_h\Lambda_h\mu_h B^2\beta_{hh}A\mu_v K - 4K\mu_h\mu_v B^2\omega^2\gamma f\beta_{hv}\alpha_h\Lambda_h \\
&\quad +4K\mu_h\mu_v B^3\beta_{hv}\omega\alpha_h\Lambda_h - 4K^2\mu_h\mu_v^2B^3\beta_{hh}\omega A - 4K\mu_h\mu_v B^3\beta_{hv}\omega\alpha_h\Lambda_h \\
&\quad +4K^2\mu_h\mu_v^2B^2\omega^2\gamma f\beta_{hh}A + 4K\mu_h\mu_v B^2\omega^2\gamma f\beta_{hv}\alpha_h\Lambda_h + 4K^2\mu_h^2\mu_v^2B^4 \\
&\quad +4K^2\mu_h^2\mu_v^2B^3\gamma f\omega - 4\omega^2\alpha_h\Lambda_h\mu_h B^2\beta_{hh}A\mu_v K - 4\omega^2\alpha_h^2\Lambda_h^2\mu_h B^2\beta_{hv} \\
&\quad -4K\mu_h^2\mu_v B^3\omega\alpha_h\Lambda_h + 4\omega^2\alpha_h\Lambda_h\mu_h^2B^2K\mu_v\gamma f + 4K\mu_h\mu_v B\omega^3\gamma f\beta_{hh}A\alpha_h\Lambda_h \\
&\quad +4\omega^3\alpha_h^2\Lambda_h^2\mu_h B\beta_{hv}\gamma f \\
&= 4\omega^3\alpha_h^2\Lambda_h^2\mu_h B\beta_{hh}A + 4\omega^2\alpha_h\Lambda_h\mu_h B^2\beta_{hh}A\mu_v K + 4K^2\mu_h\mu_v^2B^2\omega^2\gamma f\beta_{hh}A \\
&\quad +4K\mu_h\mu_v B\omega^3\gamma f\beta_{hh}A\alpha_h\Lambda_h > 0.
\end{aligned}$$

Looking at I_h^* as a function of the human shedding rate α_h (i.e. $I_h^* = I_h^*(\alpha_h)$), it can be shown in the similar manner that $I_h^*(\alpha_h)$ is an increasing function of the shedding rate α_h. Thus, following theorem is straightforward.

Theorem 4.2 *The infected component $I_h^* = I_h^*(\beta_{hv})$ of the endemic equilibrium point is a strictly monotonic increasing function on the interval $0 \leq \beta_{hv} < \infty$. Similarly, the infected component $I_h^* = I_h^*(\alpha_h)$ of the endemic equilibrium point is a strictly monotonic increasing function on the interval $0 \leq \alpha_h < \infty$. Moreover, $I_h^*(\beta_{hv} = 0) = I_h^*(\alpha_h = 0) = \bar{I}_h$ which is the infected component of the unique endemic equilibrium point P_h^* in Eq. (3.9)-(3.12).*

The relevance of Theorem 4.2 is that it suggests a clear answer to the research question which has motivated this work, by highlighting the detrimental effect of the environmental contamination on the transmission of EVD. More specifically, Theorem 4.2 in conjunction with the inequality $\mathcal{R}_0^{env} > \mathcal{R}_0^h$, show that not only the indirect contamination will increase the basic reproduction number (thus, the fast spreading of the disease), but the severity of the disease by increasing the endemic level ($\bar{I}_h(\beta_{hv}) \geq I_h^*$).

5 Numerical simulations

In this section, we present numerical simulations to support the theory presented in the previous sections and numerically assess the effect of the environmental contamination. The simulations are implemented in MatLab. The parameters values for human-human transmission are mostly taken from [46,47,56], while almost all the parameters values for environment-to-human-environment transmission have been assumed.

5.1 Sensitivity analysis

We have carried out the sensitivity analysis to determine the model's robustness to parameter values. This helps to identify the parameters that are most influential in determining disease dynamics [15]. A Latin Hypercute Sampling (LHS) scheme [8,37] samples 1000 values for each input parameter using a uniform distribution over the range of biologically realistic values, with descriptions and references given in Table 2. Using system (2.9) and a time period of 500 months, 1000 model simulations are performed by randomly pairing sampled values for all LHS parameters. Five outcome measures are calculated for

Parameters	Range	Values	Units	Source
Λ_h	Variable	100	$indiv.day^{-1}$	N/A
μ_h	0-1	0.33	day^{-1}	[56]
μ_v	0-1	0.85	day^{-1}	Assumed [7,42]
$\xi_h = 1/\tau_h$	0-1	1/4	day^{-1}	[46,56]
τ_h	1-7	4	day	[46,56]
ν_h	1-5	1.2	day^{-2}	Assumed
ω	1/2-1/21	1/21	day^{-1}	[21,47]
γ	1/7-1/14	1/14	day^{-1}	[56]
α_h	10-100	50	$cells.(ml.day.indiv)^{-1}$	[6]
$\theta_h = 1/r_h$	1/81-1	1/61	day^{-1}	[47]
r_h	1-81	61	day	[47]
f	0.4-0.9	0.70	unitless	[48,47,56]
K	10^6-10^9	10^6	$cells.ml^{-1}$	[6]
β_{hh}	0-1		day^{-1}	Variable
β_{hv}	0-1		day^{-1}	Variable

Table 2 Numerical values for the parameters of model system (2.9).

each run: susceptible individuals, exposed individuals to EVD, infectious individuals, recovered individuals and the virus concentration over the model's time span. Partial Rank Correlation Coefficients (PRCC) and corresponding p-values are computed. An output is assumed sensitive to an input if the corresponding PRCC is less than -0.50 or greater than $+0.50$, and the corresponding p-value is less than 5%.

The results are displayed in Table 3 to Table 8.

	PRCCs and significance				
Parameters	S_h	E_h	I_h	R_h	V
Λ_h	0.96^{**}	0.013	−0.0016	−0.11	0.014
μ_h	-1^{**}	-1^{**}	-0.88^{**}	-0.54^{**}	-0.25^{**}
ν_h	0.1	−0.044	0.022	−0.11	-0.79^{**}
τ_h	−0.026	−0.1	0.032	0.18^{*}	0.045
ξ_h	−0.07	−0.066	0.093	0.01	−0.061
ω	−0.026	−0.056	−0.067	−0.022	−0.058
γ	-0.57^{**}	-0.98^{**}	0.99^{**}	0.92^{**}	0.9^{**}
α_h	0.041	0.12	−0.075	0.66^{**}	−0.0063
r_h	0.046	−0.0023	−0.004	−0.03	0.9^{**}
θ_h	0.12	0.073	0.04	0.041	0.12
f	0.15^{*}	0.021	0.031	−0.039	0.055
K	−0.055	0.1	0.048	-0.91^{**}	−0.1
β_{hh}	$-6.9e-005$	−0.05	0.014	0.054	−0.015
β_{hv}	-0.54^{**}	0.37^{**}	−0.0093	−0.075	−0.12
μ_v	0.071	0.1	0.016	0.006	−0.063
$dummy$	−0.033	0.15^{*}	−0.1	-0.17^{*}	0.084

Table 3 PRCCs of model's parameters at time t = 4 days

5.2 General dynamics

In this subsection, we numerically illustrate the asymptotic behavior of the full model and the sub-model without the environment compartment. The GAS of the disease-free

Parameters	PRCCs and significance				
	S_h	E_h	I_h	R_h	V
Λ_h	0.94^{**}	-0.01	0.053	-0.037	0.012
μ_h	-1^{**}	-1^{**}	-0.93^{**}	-0.86^{**}	-0.71^{**}
ν_h	-0.05	-0.021	-0.035	-0.12	-0.72^{**}
τ_h	-0.0026	-0.064	0.041	0.12	0.0006
ξ_h	-0.033	-0.086	0.042	0.043	-0.049
ω	0.065	-0.068	-0.014	-0.018	-0.069
γ	-0.72^{**}	-0.97^{**}	0.94^{**}	0.87^{**}	0.9^{**}
α_h	0.016	0.077	-0.11	0.55^{**}	-0.016
r_h	0.12	-0.074	-0.077	-0.062	0.91^{**}
θ_h	0.018	0.015	0.035	0.019	0.13
f	0.088	0.016	0.064	-0.026	0.027
K	-0.087	0.062	0.009	-0.87^{**}	-0.14
β_{hh}	-0.081	-0.0005	-0.018	0.079	-0.1
β_{hv}	-0.79^{**}	0.79^{**}	0.0096	-0.0052	-0.071
μ_v	0.019	0.069	-0.0032	-0.0087	-0.028
$dummy$	0.0011	0.094	-0.15^{*}	-0.15^{*}	0.047

Table 4 PRCCs of model's parameters at time t = 15 days

Parameters	PRCCs and significance				
	S_h	E_h	I_h	R_h	V
Λ_h	0.89^{**}	0.11	0.064	0.036	0.023
μ_h	-0.99^{**}	-0.99^{**}	-0.97^{**}	-0.96^{**}	-0.87^{**}
ν_h	-0.12	-0.022	-0.068	-0.13	-0.79^{**}
τ_h	-0.049	-0.015	0.026	0.072	0.016
ξ_h	-0.074	-0.043	0.05	0.092	-0.03
ω	-0.0052	-0.15^{*}	0.023	-0.041	-0.054
γ	-0.56^{**}	-0.93^{**}	0.9^{**}	0.84^{**}	0.85^{**}
α_h	0.015	0.034	-0.17^{*}	0.54^{**}	-0.033
r_h	0.11	-0.09	-0.095	-0.027	0.89^{**}
θ_h	-0.0039	0.11	0.013	0.006	0.09
f	0.04	-0.016	0.079	0.027	0.028
K	-0.041	-0.018	-0.038	-0.86^{**}	-0.13
β_{hh}	-0.064	0.038	0.023	0.081	-0.097
β_{hv}	-0.7^{**}	0.86^{**}	0.17^{*}	0.071	0.032
μ_v	0.0096	0.009	-0.037	-0.014	-0.043
$dummy$	0.052	0.07	-0.11	-0.14	0.014

Table 5 PRCCs of model's parameters at time t = 30 days

equilibrium P_h^0 and the LAS of endemic equilibrium P_h^* demonstrated in Theorem 3.5 and Theorem 3.8 for the model with the environmental contamination are numerically supported by Fig. 2 and Fig. 3, respectively. However, Fig. 3 further suggests the GAS of P_h^*. Figure 4 illustrates the GAS of the disease-free equilibrium X_h^0 for the free-environmental contamination sub-model (4.1) as established in Theorem 3.5, while Fig. 5 supports the stability of the endemic equilibrium P_h^* as shown in Theorem 3.8.

Parameters	PRCCs and significance				
	S_h	E_h	I_h	R_h	V
Λ_h	0.86^{**}	0.38^{**}	0.19^{*}	0.089	0.04
μ_h	-0.94^{**}	-0.99^{**}	-0.99^{**}	-0.99^{**}	-0.93^{**}
ν_h	-0.17^{*}	−0.11	−0.13	−0.1	-0.86^{**}
τ_h	−0.028	$4.9e-005$	0.016	0.03	0.06
ξ_h	−0.11	−0.065	0.014	−0.0012	−0.059
ω	−0.053	−0.061	−0.0024	−0.025	−0.0073
γ	-0.28^{**}	-0.7^{**}	0.86^{**}	0.84^{**}	0.7^{**}
α_h	0.051	−0.029	-0.26^{**}	0.5^{**}	−0.041
r_h	0.089	-0.15^{*}	−0.077	−0.031	0.79^{**}
θ_h	0.045	0.072	0.03	0.021	0.03
f	−0.0058	0.0071	0.056	0.038	−0.0029
K	−0.058	−0.11	−0.12	-0.88^{**}	−0.1
β_{hh}	−0.031	0.023	0.0039	−0.018	−0.11
β_{hv}	-0.5^{**}	0.84^{**}	0.57^{**}	0.24^{**}	0.14
μ_v	−0.018	0.017	0.041	−0.0075	−0.025
dummy	0.0027	0.097	−0.074	−0.1	0.0062

Table 6 PRCCs of model's parameters at time t = 60 days

Parameters	PRCCs and significance				
	S_h	E_h	I_h	R_h	V
Λ_h	0.88^{**}	0.34^{**}	0.32^{**}	0.12	0.048
μ_h	-0.9^{**}	-0.98^{**}	-0.99^{**}	-1^{**}	-0.92^{**}
ν_h	−0.11	−0.072	-0.19^{*}	−0.13	-0.86^{**}
τ_h	−0.053	0.0068	0.014	−0.0015	0.098
ξ_h	−0.12	−0.087	−0.023	−0.0091	−0.066
ω	−0.12	−0.021	−0.024	−0.042	0.0067
γ	-0.22^{**}	-0.38^{**}	0.8^{**}	0.83^{**}	0.52^{**}
α_h	0.016	−0.089	-0.3^{**}	0.4^{**}	−0.041
r_h	0.046	−0.083	−0.11	−0.052	0.64^{**}
θ_h	0.042	0.039	−0.0061	0.063	0.0012
f	−0.051	−0.038	0.039	0.069	−0.043
K	−0.1	−0.11	−0.13	-0.87^{**}	−0.077
β_{hh}	0.052	0.048	0.027	−0.039	−0.13
β_{hv}	-0.42^{**}	0.84^{**}	0.74^{**}	0.48^{**}	0.16^{*}
μ_v	−0.056	0.017	0.0018	−0.0081	−0.0073
dummy	−0.031	0.076	−0.022	−0.045	0.03

Table 7 PRCCs of model's parameters at time t = 90 days

5.3 Impact of the contaminated environment on the endemic level of EVD

Herein, we numerically assess the impact of the contaminated environment on the dynamical transmission of Ebola.

Now, let us analyze the basic reproduction number $\mathcal{R}_0^{env}$. The following numerical results demonstrate the role of β_{hv} and α_h on the basic reproduction number $\mathcal{R}_0^{env}$. We begin by investigating how the basic reproduction number $\mathcal{R}_0^{env}$ depends on β_{hv} and α_h. The illustration in Fig. 6 shows that, an increase in β_{hv} and α_h results to an increase in $\mathcal{R}_0^{env}$. This latter figure also illustrates that for the chosen parameter values, if β_{hv} does not exceed 0.5 ($\beta_{hv} < 0.5$),

Sensitivity index	Parameters with significant sensitivity index		
(A) *Sensitivity analysis of Susceptible individuals S_h as output of interest*			
	Day4	Day15	Day30
PRCC	$\mu_h(-), \Lambda_h, \gamma(-), \beta_{hv}(-),$	$\mu_h(-), \Lambda_h, \beta_{hv}(-), \gamma(-),$	$\mu_h(-), \Lambda_h, \beta_{hv}(-), \gamma(-),$
(B) *Sensitivity analysis of Exposed individuals E_h as output of interest*			
	Day4	Day15	Day30
PRCC	$\mu_h(-), \gamma(-), \beta_{hv},,$	$\mu_h(-), \gamma(-), \beta_{hv},,$	$\mu_h(-), \gamma(-), \beta_{hv},,$
(C) *Sensitivity analysis of Infected individuals I_h as output of interest*			
	Day4	Day15	Day30
PRCC	$\gamma, \mu_h(-),,,$	$\gamma, \mu_h(-),,,$	$\mu_h(-), \gamma,,,$
(D) *Sensitivity analysis of Recovered individuals R_h as output of interest*			
	Day4	Day15	Day30
PRCC	$\gamma, K(-), \alpha_h, \mu_h(-),$	$K(-), \gamma, \mu_h(-), \alpha_h,$	$\mu_h(-), K(-), \gamma, \alpha_h,$
(E) *Sensitivity analysis of Free virus individuals V as output of interest*			
	Day4	Day15	Day30
PRCC	$r_h, \gamma, \nu_h(-), \mu_h(-),$	$r_h, \gamma, \nu_h(-), \mu_h(-),$	$r_h, \mu_h(-), \gamma, \nu_h(-),$

Table 8 PRCCs results for the model

then EVD can be controlled irrespective of the value of α_h. The infection will equally persist for $\beta_{hv} > 0.5$. To add more evidence on the role of the contaminated environment, Fig. 7 shows the basic reproduction numbers $\mathcal{R}_0^{env}$ and $\mathcal{R}_0^h$ versus the effective contact rate between susceptible and infected human individuals β_{hh} for $\beta_{hv} = 0.1$ and the effective contact rate between susceptible human individuals and Ebola viruses β_{hv} for $\beta_{hh} = 0.2$ when $\Lambda_h = 500$, $\mu_h = 0.033$, $\mu_v = 0.85$, $\tau_h = 4$, $\varepsilon_h = 1/4$, $\nu_h = 1.2$, $\omega = 1/21$, $\gamma = 1/14$, $\theta_h = 1/61$, $f = 0.5$, $K = 10^6$ and $\beta_{hv} = 0.1$. It illustrates that $\mathcal{R}_0^{env}$ and $\mathcal{R}_0^h$ increases as β_{hh} increases. Also, as β_{hv} increases, $\mathcal{R}_0^{env}$ increases, while $\mathcal{R}_0^h$ remains constant.

Figure 8 is an illustration of Theorem 4.2 when the endemic levels are reached for both the model with and without the environmental contamination. This figure further shows the increasing behavior of the full model-related infectious component with respect to the indirect effective contact rate β_{hv}. Once more, this highlights the detrimental role of the contaminated environment on the transmission dynamics of EVD, for as the individuals get contaminated from the environment, the number of infected individuals reached at the endemic equilibrium increases.

Simulation results in Fig. 9 illustrate the effects of the variations of the environmental contact rate β_{hv} and the shedding rate α_h on the number of infectious individuals at endemic level I_h^*. This figure illustrates that an increase on β_{hv} and/or in the shedding rate α_h in the community will increase the prevalence of EVD cases. It suggests that, the survival of Ebola viruses in the environment may accelerate the spread of EVD in the community. Thus, the problem of biological control of the virus should be addressed in communities touched by EVD in order to reduce the burden of the disease.

6 Conclusion and discussions

In this paper, we have formulated two new mathematical models for the dynamical transmission of EVD in which the following factors are incorporated: (i) the indirect transmission via the environment, (ii) the contamination through recovered individuals, (iii) the demographic dynamics as well as the concentration of Ebola viruses in the environment, (v) the infection through contact with Ebola-deceased individuals (during funerals), (iv) the dead-mediated and the clinically recovered-mediated transmissions using fractions of infectious individuals and (vi) the virulence of the Ebola virus in Ebola-deceased individuals.

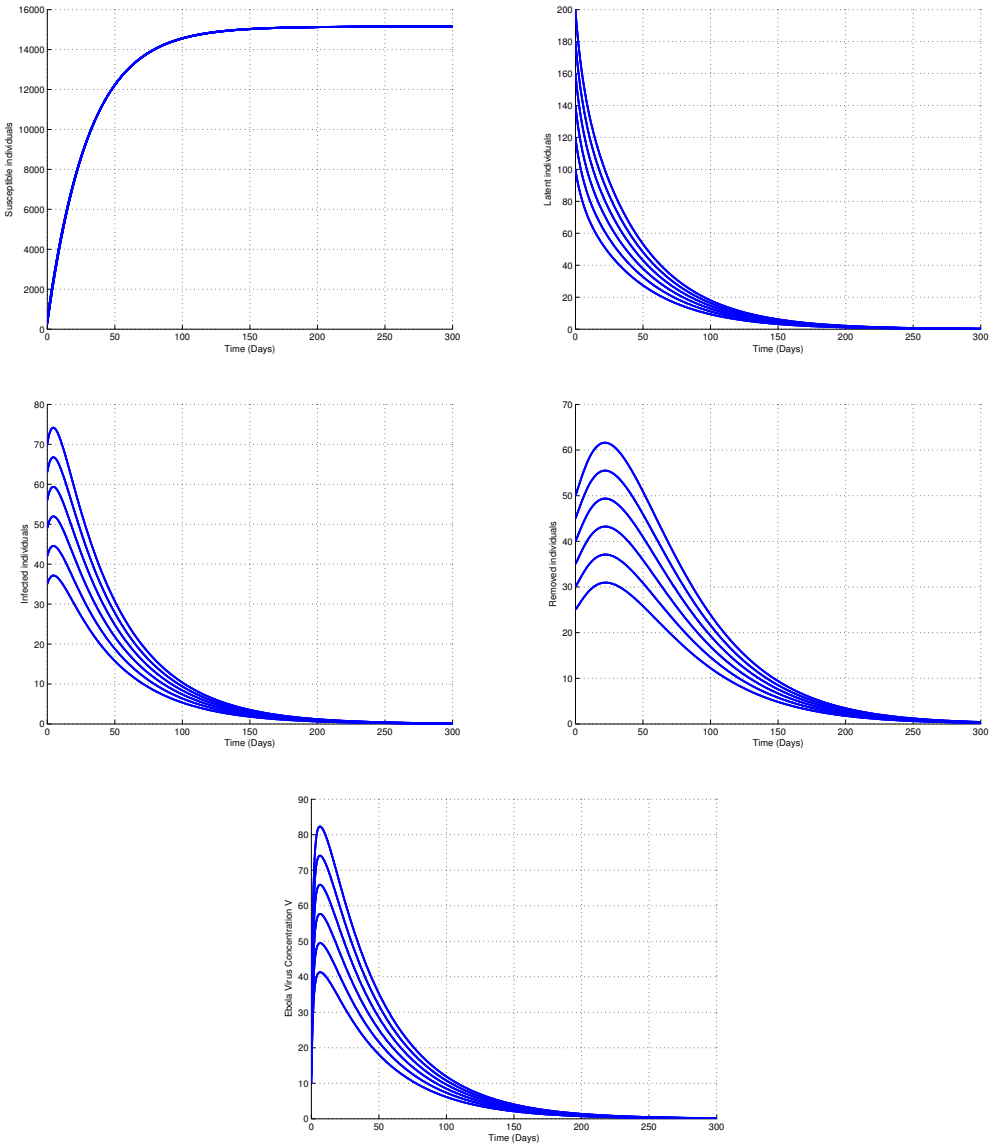

Fig. 2 GAS of the disease-free equilibrium P_h^0 when $\Lambda_h = 500$, $\mu_h = 0.033$, $\mu_v = 0.85$, $\tau_h = 4$, $\varepsilon_h = 1/4$, $\nu_h = 1.2$, $\omega = 1/21$, $\gamma = 1/14$, $\alpha_h = 0.95$, $\theta_h = 1/61$, $f = 0.5$, $K = 10^6$, $\beta_{hh} = 0.1$ and $\beta_{hv} = 0.02$ (so that $\mathcal{R}_0^{env} = 0.582 < 1$).

A qualitative analysis of the model has been presented and our main findings on the long run of the system can be summarized as follows.

(1) The disease-free equilibrium for the full model is GAS whenever the corresponding threshold quantity $\mathcal{R}_0^{env}$ is less than or equal to unity.
(2) In the case $\mathcal{R}_0^{env} > 1$, there exists a unique globally asymptotically stable endemic equilibrium for the full model.
(3) For the model without the environmental contamination, the corresponding disease-free equilibrium is GAS when the corresponding basic reproduction number $\mathcal{R}_0^h$ is less than or equal to unity.

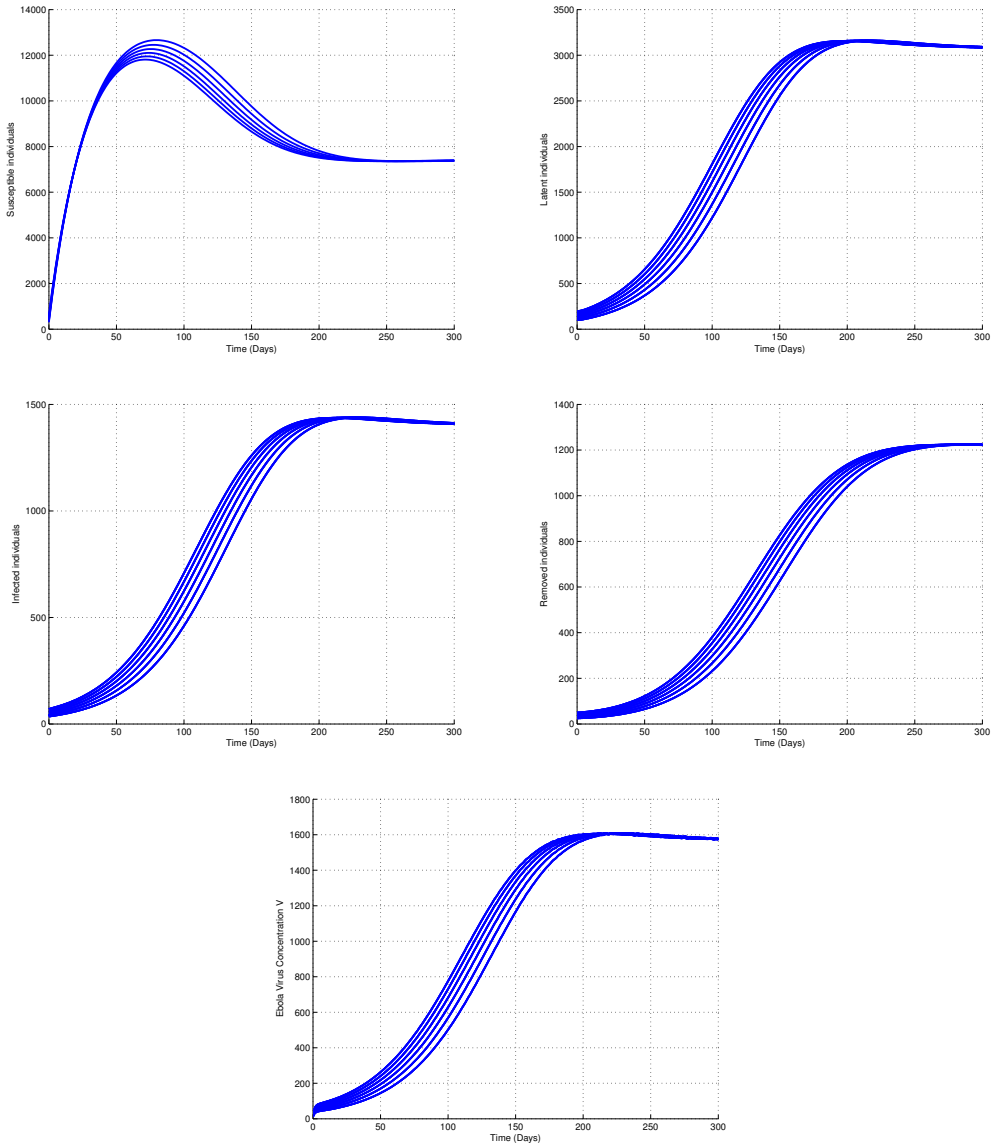

Fig. 3 Stability of the endemic equilibrium P_h^* when $\Lambda_h = 500$, $\mu_h = 0.033$, $\mu_v = 0.85$, $\tau_h = 4$, $\varepsilon_h = 1/4$, $\nu_h = 1.2$, $\omega = 1/21$, $\gamma = 1/14$, $\alpha_h = 0.95$, $\theta_h = 1/61$, $f = 0.6$, $K = 10^6$, $\beta_{hh} = 0.3$ and $\beta_{hv} = 0.03$ (so that $\mathcal{R}_0^{env} = 1.750 > 1$.)

(4) This environmental-free model exhibits a unique endemic equilibrium, which GAS whenever $\mathcal{R}_0^h > 1$.

(5) At the endemic level, for both cases in items (2) and (4) above, the number of infected individuals reached with the influence of environmental transmission is larger than the corresponding number of infected individuals in the absence of such influence.

Moreover, a quantitative investigation has been performed and the results are as follows:

- We have numerically confirmed all the theoretical results obtained with respect to the asymptotic dynamics of the model under consideration.
- The sensitivity analysis of the model has been investigated. We have found that as the time evolves, amongst others, the susceptible and infectious individuals are increasingly

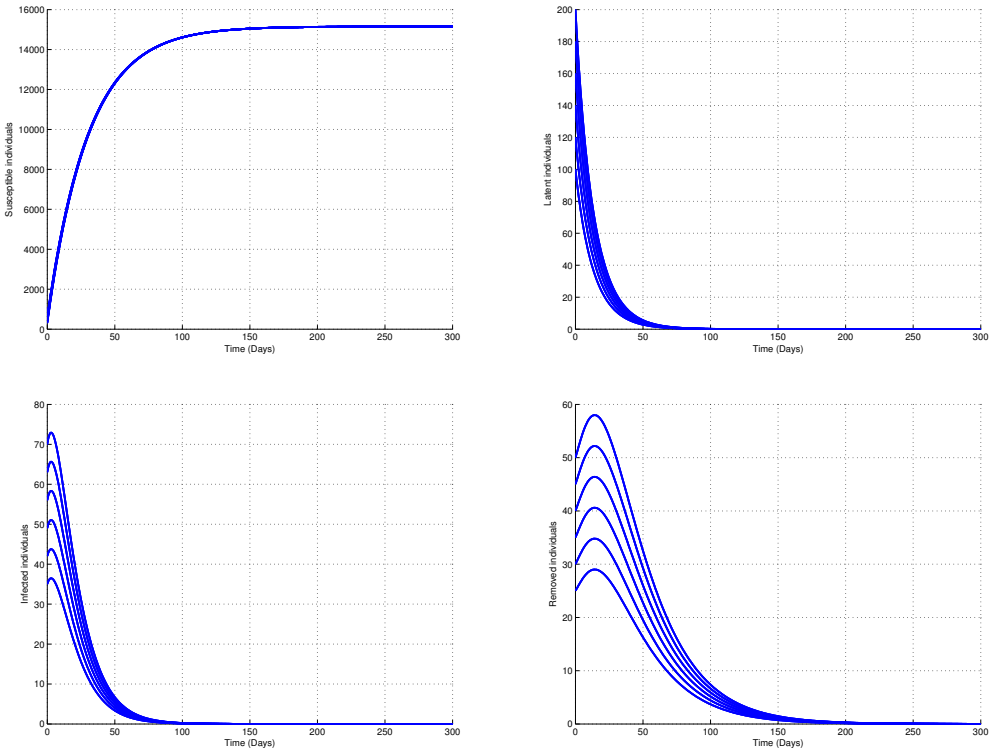

Fig. 4 GAS of the disease-free equilibrium X_h^0 when $\Lambda_h = 500$, $\mu_h = 0.033$, $\mu_v = 0.85$, $\tau_h = 4$, $\varepsilon_h = 1/4$, $\nu_h = 1.2$, $\omega = 1/21$, $\gamma = 1/14$, $\alpha_h = 0.95$, $\theta_h = 1/61$, $f = 0.6$, $K = 10^6$, $\beta_{hh} = 0.01$, $\beta_{hv} = 0.0$ (so that $\mathcal{R}_0^h = 0.058 < 1$).

sensitive to both the environmental effective contact rate and the shedding rate. This suggests a detrimental influence of the environmental contamination on the persistence and the severity of EVD and provides a negative answer to the research question under investigation.

– Throughout numerical simulations, we have found that some local stability results established theoretical can be global.

The work in [1] provided a general mathematical model for the transmission dynamics of EVD in a population stratified into two epidemiological settings: those in the community and those within the health-care system. The model incorporated traditional/cultural beliefs and customs but did not assess the impact of the environmental contamination in the transmission of EVD. Thus, a reasonable extension of our work will be to add the environmental contamination in [1], even though the mathematical analysis will become more complicated.

Appendix. Proof of Theorem 3.8

To establish Theorem 3.8 when $\mathcal{R}_0^{env} > 1$ which shows the local stability of subsystem (2.9), we used the center manifold theory proposed in [13]. To this end, we introduce the following change of variables: $x_1 = S_h$, $x_2 = E_h$, $x_3 = I_h$, $x_4 = R_h$, $x_5 = V$. Therefore, $x_1' = S_h'$, $x_2' = E_h'$, $x_3' = I_h'$, $x_4' = R_h'$, $x_5' = V'$. The disease-free equilibrium of subsystem (2.9) becomes $x_0^* = (\Lambda_h/\mu_h, 0, 0, 0, 0)$.

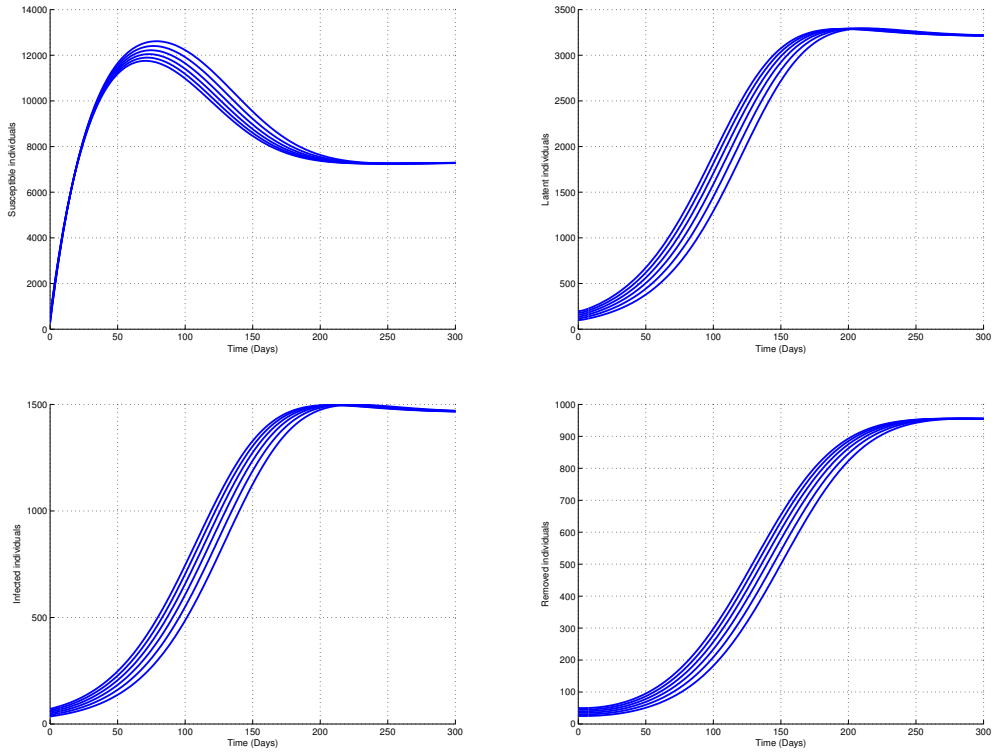

Fig. 5 Stability of the endemic equilibrium $\overline{P}_h$ when $\Lambda_h = 500$, $\mu_h = 0.033$, $\mu_v = 0.85$, $\tau_h = 4$, $\varepsilon_h = 1/4$, $\nu_h = 1.2$, $\omega = 1/21$, $\gamma = 1/14$, $\alpha_h = 0.95$, $\theta_h = 1/61$, $f = 0.6$, $K = 10^6$, $\beta_{hh} = 0.3$ and $\beta_{hv} = 0.0$ (so that $\mathcal{R}_0^h = 1.774 > 1$.

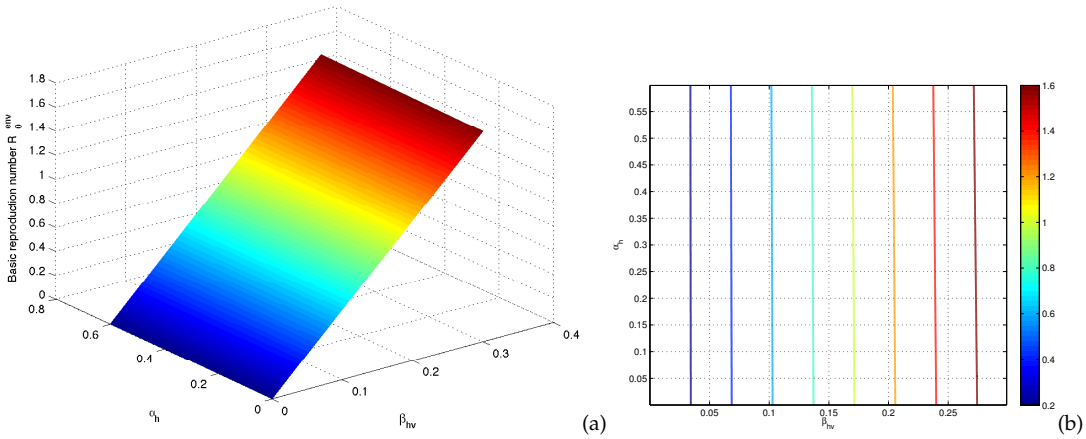

Fig. 6 (a) 3-D and (b) contour plot showing the effects of β_{hv} and α_h on the basic reproduction number $\mathcal{R}_0^{env}$ when , $\Lambda_h = 500$ $\mu_h = 0.033$, $\mu_v = 0.85$, $\tau_h = 4$, $\varepsilon_h = 1/4$, $\nu_h = 1.2$, $\omega = 1/21$, $\gamma = 1/14$, $\theta_h = 1/61$, $f = 0.5$, $K = 10^6$ and $\beta_{hh} = 0.2$.

Let $\sigma_v > 0$ be the non-negative real numbers such that $\beta_{hv} = \sigma_v \beta_{hh}$, , then the basic reproduction number $\mathcal{R}_0^{env}$ becomes

$$\mathcal{R}_0^{env} = \frac{\beta_{hh}\left(\Phi_h \omega K \mu_h \mu_v + \alpha_h \sigma_v \Lambda_h \omega\right)}{K \mu_h \mu_v (\mu_h + \omega)(\mu_h + \gamma)}.$$

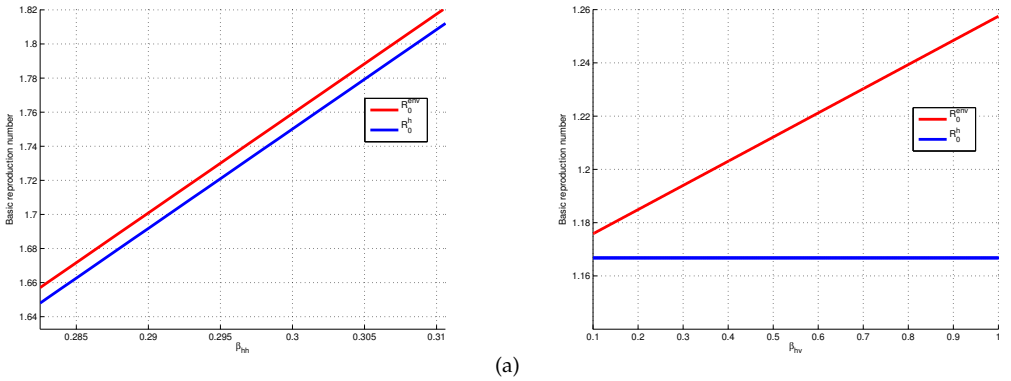

(a) (b)

Fig. 7 $\mathcal{R}_0^{env}$ and $\mathcal{R}_0^h$ versus (a) the effective contact rate between susceptible and infected individuals β_{hh} for $\beta_{hv} = 0.2$ and (b) the effective contact rate between susceptible individuals and Ebola viruses β_{hv} for $\beta_{hh} = 0.2$. For both figures, $\Lambda_h = 500$, $\mu_h = 0.0033$, $\mu_v = 0.85$, $\tau_h = 4$, $\varepsilon_h = 1/4$, $\nu_h = 1.2$, $\omega = 1/21$, $\gamma = 1/14$, $\theta_h = 1/61$, $f = 0.5$, $K = 10^6$ and $\alpha_h = 0.95$.

Let $\beta_{hh} = \phi$ be the bifurcation parameter, then solving the equation $R_0^{env} = 1$ for β_{hh} yields

$$\beta_{hh} = \phi = \beta_{hh}^* = \frac{K\mu_h\mu_v(\mu_h+\omega)(\mu_h+\gamma)}{\Phi_h\omega K\mu_h\mu_v + \alpha_h\sigma_v\Lambda_h\omega}.$$

Notice that $\mathcal{R}_0^{env} > 1$ if and only if $\beta_{hh} > \beta_{hh}^*$.

With these notations, system (2.9) takes the form:

$$\begin{cases} f_1 := x_1'(t) = \Lambda_h - \dfrac{\phi\Phi_h x_1 x_3}{x_1+x_2+x_3+x_4} - \dfrac{\phi\sigma_v x_1 x_5}{K+x_5} - \mu_h x_1, \\ f_2 := x_2'(t) = \dfrac{\phi\Phi_h x_1 x_3}{x_1+x_2+x_3+x_4} + \dfrac{\phi\sigma_v x_1 x_5}{K+x_5} - (\mu_h+\omega)\, x_2, \\ f_3 := x_3'(t) = \omega x_2 - (\mu_h+\gamma)\, x_3, \\ f_4 := x_4'(t) = \gamma(1-f)x_3 - \mu_h x_4, \\ f_5 := x_5'(t) = \alpha_h x_3 - \mu_v x_5. \end{cases} \tag{6.1}$$

The Jacobian matrix of subsystem (6.1) at the disease-free equilibrium x_0^* when $\phi = \phi^*$ is

$$J_{\phi^*} = \begin{pmatrix} -\mu_h & 0 & -\phi^*\Phi_h & 0 & -\dfrac{\phi^*\sigma_v\Lambda_h}{\mu_h K} \\ 0 & -(\mu_h+\omega) & \phi^*\Phi_h & 0 & \dfrac{\phi^*\sigma_v\Lambda_h}{\mu_h K} \\ 0 & \omega & -(\mu_h+\gamma) & 0 & 0 \\ 0 & 0 & \gamma(1-f) & -\mu_h & 0 \\ 0 & 0 & \alpha_h & 0 & -\mu_v \end{pmatrix}.$$

It is straightforward that the transformed system (6.1), with $\phi = \phi^*$ has a hyperbolic equilibrium point (i.e., the Jacobian matrix J_{ϕ^*} has a simple eigenvalue with zero real part (here, zero is a simple eigenvalue), and the remaining eigenvalues have negative real parts). Therefore the Center Manifold Theory [13] can applied to analyze the dynamics of subsystem (6.1) near the bifurcation parameter $\phi = \phi^*$. It is easy to see that a corresponding right-eigenvector of J_{ϕ^*} associated to the zero eigenvalue is $\mathbf{w} = (w_1, w_2, w_3, w_4, w_5)^T$, and a corresponding non-negative left-eigenvector associated to zero is given by $\mathbf{v} = (v_1, v_2, v_3, v_4, v_5)$, where

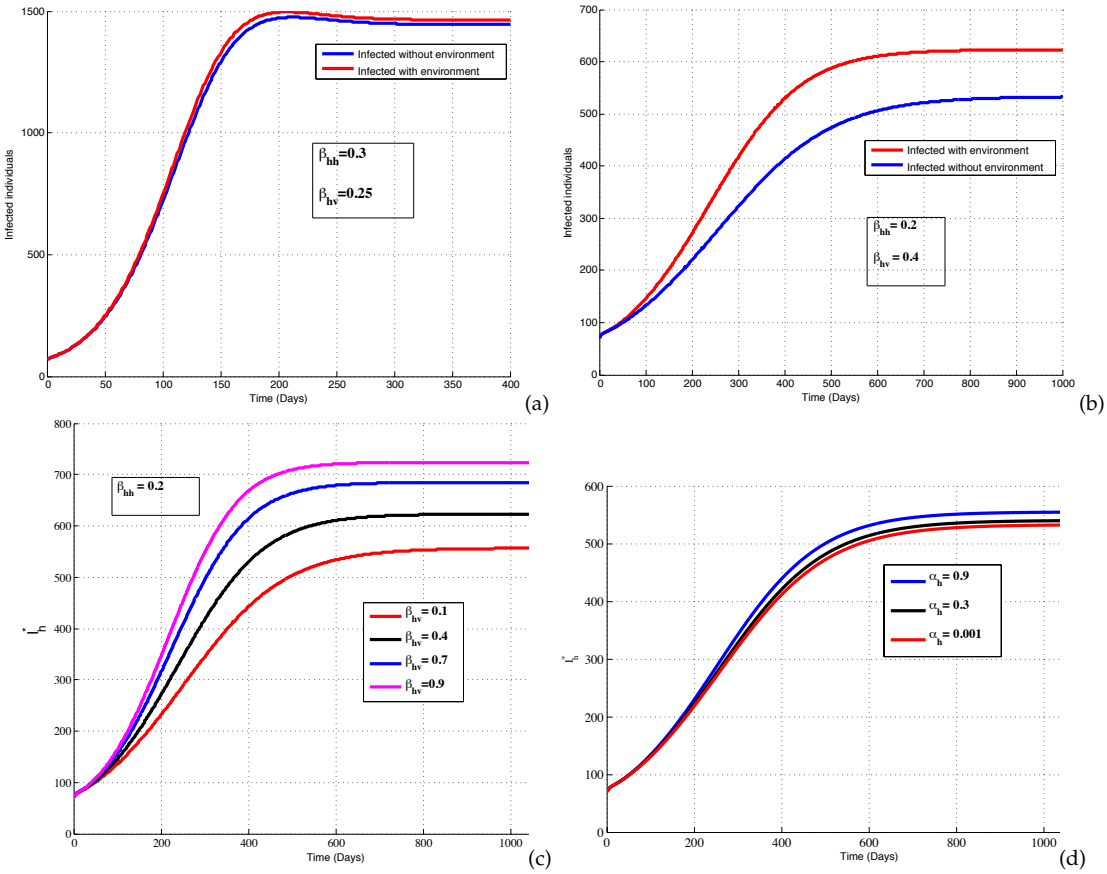

Fig. 8 Comparison of I_h^* and $\bar{I}_h$ at endemic levels when $\Lambda_h = 500$, $\mu_h = 0.033$, $\mu_v = 0.85$, $\tau_h = 4$, $\varepsilon_h = 1/4$, $\nu_h = 1.2$, $\omega = 1/21$, $\gamma = 1/14$, $\alpha_h = 0.95$, $\theta_h = 1/61$, $f = 0.5$ and $K = 10^6$. (a) Infected individuals with and without environment for two different values when $\beta_{hh} = 0.3$ and $\beta_{hv} = 0.25$ (so that $\mathcal{R}_0^h = 1.750$ and $\mathcal{R}_0^{env} = 1.774$); (b) Infected individuals with and without environment for $\beta_{hh} = 0.2$ and $\beta_{hv} = 0.4$ (so that $\mathcal{R}_0^h = 1.166$ and $\mathcal{R}_0^{env} = 1.205$); (c) I_h^* for four different values of β_{hv} when $\beta_{hh} = 0.2$; (d) I_h^* for three different values of α_h when $\beta_{hh} = 0.2$ and $\beta_{hv} = 0.1$. This is an illustration of Theorem 4.2.

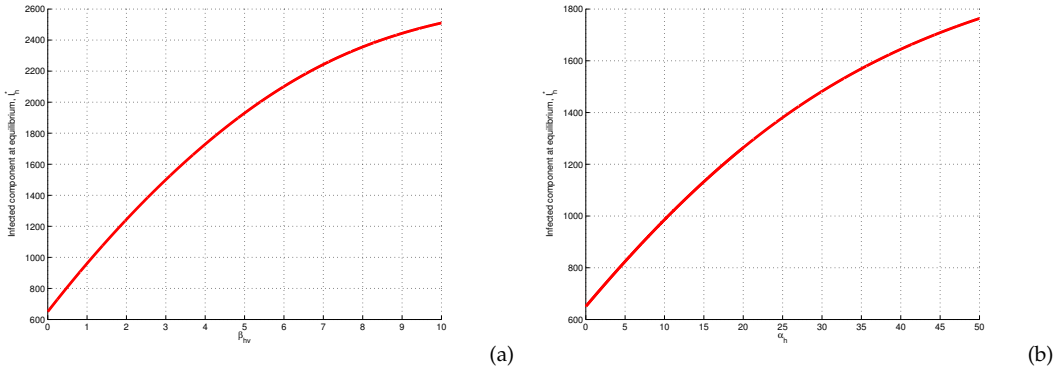

Fig. 9 I_h^* versus (a) the environmental effective contact rate β_{hv} for $\alpha_h = 0.9$ and (b) the human shedding rate α_h for $\beta_{hv} = 0.1$ when $\Lambda_h = 500$, $\mu_h = 0.033$, $\mu_v = 0.85$, $\tau_h = 4$, $\varepsilon_h = 1/4$, $\nu_h = 1.2$, $\omega = 1/21$, $\gamma = 1/14$, $\theta_h = 1/61$, $f = 0.5$, $K = 10^6$ and $\beta_{hh} = 0.2$.

$$\begin{cases} w_1 = -\mu_v(\mu_h + \omega)(\mu_h + \gamma), \\ w_2 = \mu_h\mu_v(\mu_h + \gamma), \\ w_3 = \mu_h\mu_v\omega, \\ w_4 = \mu_v\gamma(1-f)\omega, \\ w_5 = \mu_h\alpha_h\omega, \end{cases} \quad \text{and} \quad \begin{cases} v_1 = 0, \\ v_2 = \mu_h\mu_v\omega K, \\ v_3 = \mu_h\mu_v K(\mu_h + \omega), \\ v_4 = 0, \\ v_5 = \sigma_v\Lambda_h\omega. \end{cases}$$

To apply Theorem 4.1 in [13] and determine the nature and the direction of the bifurcation at $\mathcal{R}_0^{env} = 1$, we must compute the following quantities:

$$\mathbf{a} = \sum_{k,j,i=1}^{5} v_k w_i w_j \frac{\partial^2 f_k}{\partial x_i \partial x_j}(x_0^*, \phi^*); \quad \mathbf{b} = \sum_{k,i=1}^{5} v_k w_i \frac{\partial^2 f_k}{\partial x_i \partial \phi}(x_0^*, \phi^*)$$

The only non-vanishing second partial derivatives of f corresponding to the non-zero components of $\mathbf{v}$ evaluated at $\left(x_0^*, \phi^*\right)$ are:

$$\frac{\partial^2 f_2}{\partial x_2 \partial x_3}(x_0^*, \phi^*) = \frac{\partial^2 f_2}{\partial x_3 \partial x_4}(x_0^*, \phi^*) = \frac{\partial^2 f_2}{\partial x_3 \partial x_5}(x_0^*, \phi^*) = -\phi^* \Phi_h \frac{\mu_h}{\Lambda_h}$$
$$\frac{\partial^2 f_2}{\partial x_3^2}(x_0^*, \phi^*) = -2\phi^* \Phi_h \frac{\mu_h}{\Lambda_h}; \quad \frac{\partial^2 f_2}{\partial x_1 \partial x_5}(x_0^*, \phi^*) = \frac{\phi^* \sigma_v}{K}; \quad \frac{\partial^2 f_2}{\partial x_3 \partial \phi^*}(x_0^*, \phi^*) = \sigma_v.$$

Thus,

$$\begin{aligned}
\mathbf{a} &= v_2 \left[2w_1 w_5 \frac{\partial^2 f_2}{\partial x_1 \partial x_5} + 2w_3 \frac{\partial^2 f_2}{\partial x_2 \partial x_3}(x_0^*, \phi^*)\,(w_2 + w_4 + w_5) + w_3^2 \frac{\partial^2 f_2}{\partial x_3^2}(x_0^*, \phi^*) \right] \\
&= -2v_2 \left\{ -w_1 w_5 \frac{\phi^* \sigma_v}{K} + w_3 \phi^* \Phi_h \frac{\mu_h}{\Lambda_h}\,(w_2 + w_3 + w_4 + w_5) \right\} \\
&= -2v_2 \mu_h \mu_v \omega \left\{ \frac{(\mu_h + \omega)(\mu_h + \gamma)\phi^* \alpha_h \sigma_v}{K} \right\} \\
&\quad -2v_2 \mu_h \mu_v \omega \left\{ \frac{\phi^* \Phi_h \mu_h}{\Lambda_h} \left[\mu_h \mu_v (\mu_h + \gamma) + \mu_h \mu_v \omega + \mu_v \gamma (1 - f) + \mu_h \alpha_h \omega \right] \right\} < 0 \\
\mathbf{b} &= v_2 w_3 \frac{\partial^2 f_2}{\partial x_3 \partial \phi}(x_0^*, \phi^*) = \sigma_v \mu_h^2 \mu_v^2 \omega^2 K > 0.
\end{aligned}$$

Thanks to item 4 of Theorem 4.1 in [13], the endemic P_h^* of sub-model (2.9) is locally asymptotically stable when $\mathcal{R}_0^{env} > 1$, but near to 1. Moreover, the bifurcation of the subsystem (2.9) around $\mathcal{R}_0^{env} = 1$ is trans-critical. The proof is complete.

Acknowledgments

The first (T.B.) and the third (J.L.) authors are grateful to the South African Research Chairs Initiative (SARChI Chair), in Mathematical Models and Methods in Bioengineering and Biosciences. The first (T.B.) and the second (S.B.) authors acknowledge the support of Center of Excellence Cameroon (CETIC). The authors are also grateful to the three anonymous referees and to Prof Chin-Hong Park, Editor in Chief of this journal, whose, suggestions and remarks substantially improved this manuscript.

References

1. Agusto, F. B., Teboh-Ewungkem, M.I., Gumel, A. B.: Mathematical assessment of the effect of traditional beliefs and customs on the transmission dynamics of the 2014 Ebola outbreaks. BMC Medicine (2015) 13:96 DOI 10.1186/s12916-015-0318-3.
2. Althaus, C.: "Estimating the reproduction number of Ebola (EBOV) during outbreak in West Africa", PLOS Currents, 1, Sept 2, (2014).
3. Anderson, R.M., May R.M.: Infectious Diseases of Humans: Dynamics and Control. Oxford,England: Oxford University Press, (1991).
4. Arata, A.A., Johnson, B.: Approaches toward studies on potential reservoirs of viral haemorrhagic fever in southern Sudan (1977). In Ebola Virus Haemorrhagic Fever (Pattyn, S.R.S., ed.), 191-200 (1978).
5. Baize, S., Pannetier, D., Oestereich, L.: Emergence of Zaire Ebola Virus Disease in Guinea - Preliminary Report. New England Journal of Medecine (2014).

6. Bani-Yabhoub, M., et al.: Reproduction numbers for infections with free-living pathogens growing in the environment, Journal of Biological Dynamics. 6 2, 923-940 (2012).
7. Bibby, K., et al.: Ebola Virus Persistence in the Environment: State of the Knowledge and Research Needs, Environ. Sci. Technol. Lett. 2, 2-6 (2015).
8. Blower, S.-M., Dowlatabadi, H.: Sensitivity and uncertainty analysis of complex models of disease transmission: an HIV model, as an example. International Statistical Review. 2, 229-243 (1994).
9. Bray, M.: Filoviridae. In: Clinical Virology, Richman DD, Whitley RJ, Hayden FG (Eds), ASM Press, Washington, DC 2002. p.875.
10. Capasso, V., Paveri-Fontana, S. L.: A mathematical model for the 1973 cholera epidemic in the european mediterranean region, Revue dépidémioligié et de santé publiqué 27:121 (1973).
11. Carr, J.: Applications Centre Manifold Theory. Springer-Verlag, New York, (1981).
12. Castillo-Chavez, C., Thieme, H.: Asymptotically autonomous epidemic models, in: O. Arino, D. Axelrod, M. Kimmel, M. Langlais (Eds.), Mathematical Population Dynamics: Analysis of Heterogeneity, pp. 33. Springer, Berlin (1995).
13. Castillo-Chavez, C., Song, B.: Dynamical models of Tuberculosis and their applications. Math. Biosc. Eng. 1 (2) 361-404 (2004).
14. Chan, M.: Ebola Virus Disease in West Africa. http://www.cdc.gov/vhf/ebola/outbreaks/2014-west-africa/united-states-imported-case.html (Accessed on October 01, 2014).
15. Chitnis, N., Hyman, J.-M., Cushing, J.-M.: Determining important parameters in the spread of malaria through the sensitivity analysis of a mathematical model. Bull. of Math. Biol. 70, 272-1296 (2008).a-No Early End to the Outbreak, The New England Journal of Medicine. September 25, (2014), DOI: 10.1056/NEJMp1409859.
16. Chowell, G., Nishiura, N.: Transmission dynamics and control of Ebola virus disease (EVD): a review. BMC Medicine 2014, 12:196.
17. Chowell, G., et al.: The basic reproductive number of Ebola and the effects of public health measures: the cases of Congo and Uganda, Journal of Theoretical Biology 229, 119-126 (2004).
18. Codeço, C.T.: Endemic and epidemic dynamic of cholera: the role of the aquatic reservoir, BMC Infectious Diseases 1:1.
19. Diekmann, O., Heesterbeek, J. A. P., Roberts, M. G.: The construction of next-generation matrices for compartmental epidemic models. J R Soc Interface 7 873-885 (2010).
20. Ebola virus disease. Fact sheet N^0 103, Updated April 2014, http://www.who.int/mediacentre/factsheets/fs103/en/
21. Eichner, M., Dowell, S.F., Firese, N.: Incubation period of Ebola Hemorrhagic Virus subtype Zaire, Public Health Res. Perspect. 2, 1 (2011).
22. Fasina, F. O., Shittu, A., Lazarus, D., Tomori, O., Simonsen, L., Viboud, C., Chowell, G.: Transmission dynamics and control of Ebola virus disease outbreak in Nigeria, July to September 2014. Euro Surveill. 2014;19(40):pii=20920. Available online: http://www.eurosurveillance.org/ViewArticle.aspx?ArticleId=20920.
23. Feldmann, H.: Ebola - A Growing Threat? New England Journal of Medicine (2014).
24. Feldmann, H., et al.: Ebola virus ecology: a continuing mystery, Trends Microbiology. 12, 433-437 (2004).
25. Formenty, P., Hatz, C., Le Guenno, B., et al.: Human infection due to Ebola virus, subtype Côte d'Ivoire: clinical and biologic presentation. J. Infect. Dis. 179 Suppl 1:S48 (1999).
26. Groseth, A., Feldmann, H., Strong, J. E.: The Ecology of Ebola Virus. TRENDS in Microbiology, 15 (9) 408-416 (2007).
27. Ivorra, B., Ngom, D., Ramos, A. M.: Be-CoDiS: a mathematical model to predict the risk of human diseases spread between countries-validation and application to the 2014-2015 ebola virus disease epidemic. Bull. Math. Biol. (2015) 77:1668-1704, DOI 10.1007/s11538-015-0100-x.
28. Jahrling, P. B., Geisbert, T. W., Dalgard, D. W., et al.: Preliminary report: isolation of Ebola virus from monkeys imported to USA. Lancet 1990; 335:502.
29. Kuniholm, M. H.: Bat exposure is a risk factor for Ebola virus infection. In Filoviruses: Recent Advances and Future Challenges: An ICID Global Symposium (2006).
30. Lakshmikantham, L., Leela, S., Martynyuk, A. A.: Stability Analysis of Nonlinear Systems. New York: Marcel Dekker, Inc. p. 155-170 (1989).
31. Legrand, J., Grais, R.F., Boelle, P.Y., Valleron, A. J., Flahault, A.: Understanding the dynamics of Ebola epidemics, Epidemiol. Infect. 135 , 610-621 (2007).
32. Lekone, P. E., Finkenstädt, B. F.: Statistical Inference in a Stochastic Epidemic SEIR Model with Control Intervention: Ebola as a Case Study. Biometrics 62, 1170-1177 (2006).
33. Leroy, E. M., et al.: Fruit bats as reservoirs of Ebola virus. Nature, 438, 575-576 (2005).
34. Leroy, E. M., et al.: Multiple Ebola virus transmission events and rapid decline of central African wildlife, Science 303.5656, 387-390 (2004).
35. Li, M.Y., Graef, J.R., Wang, L., Karsai, J.: Global dynamics of a SEIR model with varying total population size. Math. Biosci. 160 (1999), 191–213.
36. Li, M. Y., Muldowney, J. S.: A geometrical approach to global-stability problems. SIAM J. Appl. Anal. 27, 1070-1083 (1996).
37. Marino, S., Hogue, I.-B., Ray, C.-J., Kirschner, D.-E.: A methodology for performing global uncertainty and sensitivity analysis in systems biology. J. Theor. Biol. 254, 178-196 (2008).
38. Miranda, M. E., Ksiazek, T. G., Retuya, T. J., et al.: Epidemiology of Ebola (subtype Reston) virus in the Philippines, 1996. J. Infect. Dis. 179 Suppl 1:S115 (1999).

39. Ndanguza, D., et al.: Statistical data analysis of the 1995 Ebola outbreak in the Democratic Republic of Congo. Afr. Mat. 24, 55-68 (2013) .
40. Oähea, T. J., et al.: Bat Flight and Zoonotic Viruses. Emerging Infectious Diseases. 20, 5 (2014).
41. Onyango, C. O., Opoka, M. L., Ksiazek, T.G., et al.: Laboratory diagnosis of Ebola hemorrhagic fever during an outbreak in Yambio, Sudan, 2004. J. Infect. Dis. 196 Suppl 2:S193 (2007).
42. Piercy, T. J., et al.: The survival of filoviruses in liquids, on solid substrates and in a dynamic aerosol. J. Appl. Microbiol. 109 (5), 1531-1539 (2010).
43. Pourrut, X., et al.: Spatial and temporal patterns of Zaire ebola virus antibody prevalence in the possible reservoir bat species. J. Infect. Dis. 15; 196 Suppl 2:S176-83 (2007).
44. Sanchez, A., Lukwiya, M., Bausch, D., et al.: Analysis of human peripheral blood samples from fatal and nonfatal cases of Ebola (Sudan) hemorrhagic fever: cellular responses, virus load, and nitric oxide levels. J. Virol. 78, 10370 (2004).
45. Smith, H. L., Waltman, P.: The Theory of the Chemostat. Cambridge University, (1995).
46. The Centers for Disease Control and Prevention. First imported case of Ebola diagnosed in the United States.
47. The Centers for Disease Control and Prevention. 2014 Ebola outbreak in West Africa. http://www.cdc.gov/vhf/ebola/outbreaks/2014-west-africa/index.html (Accessed on September 29, 2014).
48. Towers, S., Patterson-Lomba, O., Castillo-Chavez, C.: Temporal variations in the effective reproduction number of the 2014 West Africa Ebola outbreak, PLOS Currents Outbreaks, Sept 18, (2014).
49. Towner, J. S., Sealy, T. K., Khristova, M. L., et al.: Newly discovered ebola virus associated with hemorrhagic fever outbreak in Uganda. PLoS Pathog. 4:e1000212 (2008).
50. Tsanou Berge, S. Bowong, J. M.-S. Lubuma, Global stability of a two-patch cholera model with fast and slow transmissions, Math. Comput. Simul.(2015), In Press .
51. Tsanou Berge, Moremedi, M. G., Lubuma, J. M.-S., Morris, N., Shava, R. K.: A simple mathematical for Ebola in Africa. Under review (2015).
52. van Den Driessche, P., Watmough, J.: Reproduction numbers and sub-threshold endemic equilibria for compartmental models of desease transmission, Math. Biosci. 180, 29-48 (2002).
53. World Health Organization. Ebola response roadmap situation report, 26 September 2014. http://apps.who.int/iris/bitstream/10665/135029/1/roadmapupdate26sept14-eng.pdf?ua=1 (Accessed on September 26, 2014).
54. World Health Organization. Ebola situation in Senegal remains stable. http://www.who.int/mediacentre/news/ebola/12-september-2014/en/ (Accessed on September 12, 2014).
55. World Health Organization. Unprecedented number of medical staff infected with Ebola. http://www.who.int/mediacentre/news/ebola/25-august-2014/en/ (Accessed on August 25, 2014).
56. WHO Ebola Response Team. Ebola Virus Disease in West Africa - The First 9 Months of the Epidemic and Forward Projections. N. Engl. J. Med. (2014).
57. World Health Organization. Global Alert Response. Ebola virus disease - Democratic Republic of Congo. http://www.who.int/csr/don/2014$_0$8$_2$7_ebola/en/ (Accessed on August 28, 2014). doi: 10.1086/674795.
58. Zhang, Z., Ma, Z.: Global dynamics of an SEIR epidemic model with saturating contact rate. Math. Biosci. 185, 15-32 (2003).
59. D. Youkee et al., Assessment of environmental contamination and environmental decontamination practices within an ebola holding unit, Freetown, Sierra Leone. PLOS ONE, December 1, 2015, DOI: 10.137/journal.pone.0145167.